# The Mathematical Model for The Designing of an Aerodynamic Control System for Launch Vehicles

a project presented to
The Faculty of the Department of Aerospace Engineering
San José State University

in partial fulfillment of the requirements for the degree
***Master of Science in Aerospace Engineering***

by

**Hieu G. Trinh**

December 2024

approved by

Dr. Periklis Papadopoulos
Faculty Advisor

ABSTRACT

**The Design of an Aerodynamic Control System for Launch Vehicles**

Hieu G. Trinh

In recent years, the rise of space flights and rocket launches has skyrocketed as a revolutionary movement. While the new space age is rapidly moving forward, advanced technologies keep pushing into the future, and launch vehicles have barely changed in overall design for decades despite being a pivotal part of any space launch. The majority of launch vehicles acquire dynamic control authority from the rocket engines, gimbaled, and provide thrust vectoring that allows boosters six degrees of freedom control capability. Most of the current rocket engines are complicated and have heavy hydraulic control systems with limited actuator angles This research aims to replace that with a control package that includes aerodynamic control surfaces for the endo-atmospheric environment and RCS thrusters for exo-atmospheric environment maneuverability and agile responses for the endo-atmospheric when needed.

# Acknowledgments

I would like to express my utmost gratitude to:

- First and foremost, my mom and dad, for their unconditional love, support, and trust for everything I have done. I wouldn't have made it this far and achieved this much without them by my side.
- My advisor, Dr. Periklis Papadopoulos, for his guidance and advice throughout not only this project but also my academic career, from undergrad to now, the end of my grad school.
- My friend, Stanley Krzesniak, a friend, a secondary advisor, has been there to help and advise me from the moment I first met him and to this day when I have been working in the Aerospace/Defense industry for almost 2 years.
- All of my friends, Devin Jordao, Joseph Bruno, Stanley Krzesniak, Derek Ye, Jason Nguyen, Jesse Franklin, and Anthony Lopez for being my closest friends, and for being there for me during my hardest moments. I owe much of my success to them.
- Professor Jeanine Hunter, Dr. Long Lu, and Dr. Yawo Ezunkpe, for their inspiration, kindness, and knowledge.
- To the San Jose State University Aerospace Engineering Department faculty, for my education.
- To my co-workers at Raytheon and Lockheed Martin, for the help and the opportunity to grow.
- To my very first manager, Andrea Gutierrez at Raytheon, for the opportunity to start a career, to grow in and outside of work.
- To my team leads, Gabriel Moreno (RTX) and Stephen Byrd (LM), for the understanding, advice and guidance to success.
- To John Cancio, Kevin Ott, and Eric Lam (LM) for being supportive of me in and outside of work, and encouraging me to become a better engineer every day.

# Table of Contents

# List of Figures

# List of Tables

# 1. Introduction

## 1.1 Motivation

From the early dawn of mankind's history, humans have always had the desire to voyage and conquer the universe, reach the furthest testing all the boundaries of capabilities. Throughout time, the greatest minds in each society have been collecting data, studying, and analyzing what is far beyond the clouds. Despite all theories and efforts, it was only until the scientific breakthroughs and engineering technological advancements; humankind was finally able to achieve the earliest success during the space race of the Cold War between the world's two superpowers at the time, the Soviets made Sputnik I – world first man-made satellite to orbit the earth. The historical milestone created a ripple event from both nations leading to the first human to be sent to the edge of space the U.S.S.R and safely returned, Yuri Gagarin in Vostok 1; followed by a successful landing of mankind to the moon, Neil Armstrong from the United States boarding Saturn V, the most powerful rocket booster ever flown by a human.

Fasting forward to go back to the modern day, the space age has certainly evolved from a symbol of an armed race between two supernations that can only be designed and operated by militaries and governments to a fruitful industry is a competing marking of privately owned companies and while being operated by public government agencies. This opens many windows of opportunities for all the brightest minds all over the globe, making space launches more accessible with fewer constraints. The greatest example can be named American companies like SpaceX and Blue Origin, civilian companies were founded for innovation and operate to push the limit of imagination. In the vicinity of federal oversight and open market principles, the burgeoning space age has unfolded and bloomed to the next level propelled by unrestricted innovation and unprecedented engineering prowess. In turn, this has inspired many generations of new engineers with the hope to see, work, and contribute to human progress in conquering outer space. In the horizon of advancing new science, reducing the cost of design, manufacture, and operation is also a key part of next-generation engineering. One way to do so is re-engineering the launch vehicle, the costliest part of any space launch.

Figure 1-1 – SpaceX's Falcon 9 rocket booster landed on a drone ship [1].

For many years, the space industry has revolved around gimbaled rocket boosters, where the launch vehicle relies on the control authority of rocket engines. However, the process of

designing advanced engines for rocket boosters is a long and foremost, highly expensive process. A more cost-efficient method can be implementing aerodynamic control surfaces to assist and reduce to need of complex and expensive gimbaled rocket engines. Great examples can be guided air-launched missiles such as the AIM-9X Sidewinder and the AIM-120 AMRAAM use an aerodynamic maneuvering system instead of thrust vectors to maneuver at high accelerations or stabilize trajectories at a lower cost and less complicated design.

Figure 1-2 – L3 Harris/Aerojet Rocketdyne RS-25 rocket engine [2].

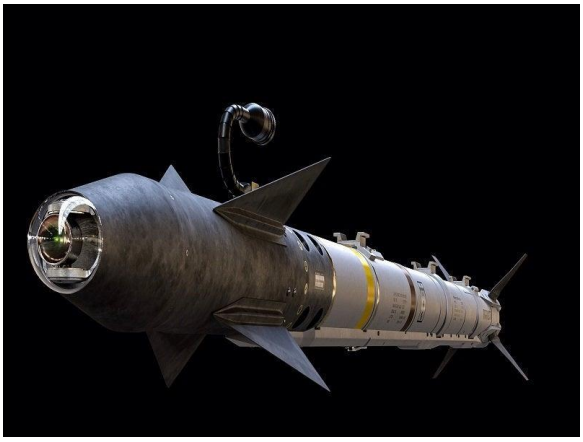

Figure 1-3 – U.S. Air Force and U.S. Navy AIM-9X Sidewinder missiles use vector-controlled fins [3].

## 1.2 **Literature Review**

This section provides literature elaboration on the current state of in-used technologies, addresses the concerns expressed previously, and the work-forward solution that can help solve the problem.

The fundamental Newton's Second Law of Motion states that the force acting on an object is equal to the mass of the object multiplied by its acceleration (F = ma). This law explains how the velocity of an object changes when it is subjected to an external force. Essentially, it shows that the greater the force applied to an object, the greater its acceleration, and that objects with larger masses require more force to achieve the same acceleration as lighter objects. This

fundamental principle is a cornerstone in the study of mechanics and helps explain the understanding of the behavior of moving objects.

Classical control includes various methods of designing optimal control techniques such as LQR control an d PID control. LQR control, or Linear Quadratic Regulator control, is an advanced optimal control technique used in the design of dynamic systems to achieve the best possible performance while minimizing a cost function. This cost function typically balances two competing objectives: minimizing the error between the system's desired and actual state and reducing the effort or energy required to control the system. LQR uses a state-space representation of the system and solves for a control law that provides feedback by multiplying the state vector by an optimal gain matrix. This results in a control input that drives the system toward stability and optimal performance. LQR is particularly effective in systems where precision and efficiency are critical, such as in aerospace, robotics, and modern control systems, where it ensures smooth and robust performance even in the presence of disturbances or uncertainties.

PID control, which stands for Proportional-Integral-Derivative control, is a widely used feedback mechanism in control systems to maintain a desired output level by continuously adjusting inputs. It works by calculating an error value as the difference between a desired setpoint and the actual process variable, then applying a correction based on three terms: proportional, integral, and derivative. The proportional term corrects the error based on its current value, the integral term addresses the accumulation of past errors, and the derivative term predicts future error trends. By tuning these three parameters, a PID controller can achieve stable, precise, and responsive control over a system, making it invaluable in various applications such as industrial automation, robotics, and process control.

There are many ways to dynamically control and stabilize airborne vehicles, from high-lift devices like slats and flaps to provide additional stability, control and generate lift and low altitude, to aerodynamic control surfaces like ailerons, elevators, and vertical stabilizers to stabilize and control the dynamical state of the plant; and lastly to thrust vectoring and gimbaled engines to provide additional control authority and maneuverability of vehicles. These different methods are used comprehensively in different air platforms such as all three for advanced fighter jets; high-lift devices and aerodynamics control surfaces for civilian aircraft. However, when it comes to rocket boosters, the most popular method to be used is thrust vectoring through gimbaled engines at the bottom of boosters to create control torque by redirecting the thrust vector [11] and [12].

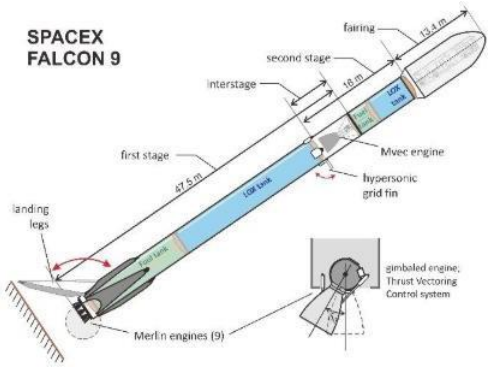


Figure 1-4 – SpaceX's Falcon 9 rocket booster and Merlin, gimbaled rocket engines [4].

A gimbaled rocket engine provides not only the lifting power but also the main dynamical controller of the launch vehicle with thrust vector control capability. The subject of review, the Falcon 9 rocket booster utilizes a Merlin rocket engine, gimbaled that can provide the overall system with thrust vector control capability in six degrees of freedom (6-DOF). The simulation model of the system can be built dynamically in MATLAB/Simulink including propulsion, aerodynamics, environmental, weight, and thrust vector control [4]. To begin, it is essential to start with a mathematical model representing the dynamic model of the booster to validate the correct behaviors of the system.

The Falcon 9's mathematical model consists of the modeling of subsystems such as environment, controller, equation of motion, rocket, and result and display subsystems model in Simulink. Firstly, the equations of motion can be used to represent all six degrees of freedom of the overall system [4].

$$\dot{\mathbf{V}}_b = \frac{F_b}{m} - \boldsymbol{\omega} \times \mathbf{V}_b \quad (1.1)$$

$$\dot{\overline{\omega}}\, I^{-1} = [\overline{M}_b - \overline{\omega} \times I\overline{\omega} - I\dot{\overline{\omega}}] \quad (1.2)$$

In which,

$\overline{V}_b$ : Velocity (translational) vector on the body axes.
$\overline{\omega}$ : Rotational rate vector (angular velocity).
$\overline{F}_b$ : Forces vector, acting on the body axes.
$\overline{M}_b$ : Moments vector, acting on the body axes.
m : Mass.
I : Moment of Inertia tensor.

Elaborating the equation of motion further, angular velocity can be expressed by Euler angles such as roll, pitch, and yaw rates for a state-space form conversion and rotating matrix for better implementation into Simulink modeling.

Additional characteristics of the rocket booster are also required for better modeling of the system, such as operation envelope and first-stage fuel mass flow rate, 273.3 kg/s with 165.6s of burning time and second-stage mass flow rate, 273.3 kg/s and a total burn time of 392.5s [5]. Being the gimbaled rocket system, the control system consists of a thrust vector control model

and the launch vehicle's attitude control system with thrust ignition and jettison schedules [4]. The model has been simplified with only longitudinal plane control, where there are only translational motions in the X and Z axes, which provide moments of pitch and roll while the yawing moment remains zero [10].

Since the dynamic state of the launch vehicle is non-linear coupled with time-varying variables such as aerodynamic and inertial, linearization is a must to apply linear control techniques [11]. Hence the presence of gain scheduling, and controller gains of different linearized models at different phases of flight [13]. Control techniques such as Proportional-Integrative-Derivative (PID) or pole placement are quite popular in real-world applications and well recognized as seen in [4], [11], [12], and [14]. PID controller with its popularity also has many downsides in the robustness of the model uncertainty and external disturbances rejection [11]. However, a better degree of robustness and a (sub-)optimal trajectory tracking solution can be ensured using optimal controllers in the linear domain such as the Linear Quadratic Regulator (LQR) [11]. With its robustness, LQR can be used to address the attitude control problem or state estimation and control [11], [15] and [16]

Furthermore, a more complex booster clustered launched vehicle with an additional motor configured in a clustered booster system such as SpaceX's Falcon Heavy or NASA's Space Launch System (SLS) operates similarly with a different dynamic model. The clustered booster system dynamical model can be simplified into a simulation model of multi-beam with the following assumptions [6]:

- Connection points between core and side boosters are rigid connections.
- No elastic deformation occurs at the connection point of the booster.
- Elastic deformation of core and boosters is small and negligible.
- Torsional deformation can be ignored.
- The inertia force caused by the rotation of the earth can be ignored.
- The change of the center of mass has no correlation with the elastic deformation.

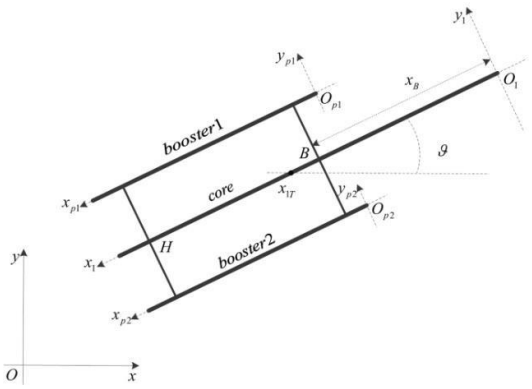


Figure 1-5 – Multi-beam model of clustered booster launch system [6].

It can be easily overlooked that a rocket booster and its internal liquid fuel have a strong coupled relationship with each other, where changes in the dynamic of the booster would cause its liquid fuel to become dynamic; which further causes more vibration that would be picked up by the sensor as the overall model of the system being updated, which in turn provides

compensation to the system and furthermore changes the dynamical state of the liquid fuel and the cycle repeats. Beyond, while in motion, the dynamic state of the system costs liquid propellants to become dynamic, together coupled as a spring-mass system or a combined spring-damper-mass system [6], [7] and [8].

Removing the gimbaled nozzle of the engine limits the ability to provide attitude control authority. At lower altitudes with much denser air, any Aerodynamic Maneuvering System (AMS) such as fins, or control surfaces can sufficiently control. However, the higher the booster travels, the more insufficient AMS becomes, with the extension to the exo-atmospheric environment. Therefore, an attitude determination control system (ADCS) often complements the AMS with quick and short pulses that provide attitude control capabilities. Examples include the Russian K-300P Bastion-P missile and the American Patriot missile both use an attitude control system to adjust the initial heading angle and proper flight attitude. The two missile systems use multiple fast, single-pulse solid rocket motors for proper attitude control within a short period of time. On the other hand, spacecraft and satellites also use the method with a slight difference in using liquid fuel with mini thrusters instead of single-pulse solid rocket engines for various reasons such as controllability. Therefore, it would be comprehensive to review the differences in the design of an ADCS to see the pros and cons of solid rocket engines or liquid propellants.

Figure 1-6 – The Russian K-300P Bastion P missile is launched vertically, and an attitude control system is used to adjust the heading angle [23].

Figure 1-7 – The American Lockheed Martin Patriot PAC-3 missile engages an attitude control system to adjust the heading angle after launch [24].

Besides using RCS for exo-atmospheric conditions, there is another method to be utilized for active control, which is more popular within spacecraft and satellites, the reaction wheels. The reaction wheel's highly reactive nature in addition to the ability to output continuous feedback control makes this method very effective for the operational envelopes of spacecraft. Reaction wheels would create torques internally within the spacecraft, offering the ability to control the attitude contributions such as roll, pitch, and yaw via momentum from reaction wheels.

Table 1-1 – Reaction Control System (RCS) and Attitude Control Thrusters [20]

| **Company** | **Model** | **Isp (s)** | **Thrust range (N)** | **Mass (kg)** |
|---|---|---|---|---|
| Marotta | CGMT | N/A | 0.1 – 10 N | 0.60 |
| Aerojet Rocketdyne | MR-401 | 184 – 180 | 0.07 – 0.09 | 0.60 |
| Aerojet Rocketdyne | MR-103G | 224 – 202 | 0.19 – 1.13 | 0.33 |
| Aerojet Rocketdyne | MR-103J | 229 – 219 | 0.19 – 1.13 | 0.37 |
| Aerojet Rocketdyne | MR-111G | 229 – 219 | 1.8 – 4.9 | 0.37 |
| Aerojet Rocketdyne | MR-106L | 235 – 228 | 4 – 10 | 0.59 |

| | | | | |
|---|---|---|---|---|
| Aerojet Rocketdyne | MR-107T | 225 – 222 | 54 – 125 | 1.01 |
| Aerojet Rocketdyne | MR-107S | 236 – 225 | 85 – 360 | 1.01 |
| Aerojet Rocketdyne | MR-107U | 229 – 223 | 182 – 307 | 1.38 |
| Aerojet Rocketdyne | MR-107V | 229 – 223 | 67 – 220 | 1.01 |
| Aerojet Rocketdyne | MR-104H | 237 – 22 | 201 – 554.2 | 2.40 |
| Aerojet Rocketdyne | MR-104J | 223 – 215 | 440 – 614 | 6.44 |
| Aerojet Rocketdyne | MR-80B | 225 – 200 | 31 – 3630 | 168 |

Spacecraft attitude determination and control systems are critical for the accurate orientation of satellites and other space vehicles. The latest progress in attitude determination has benefited from advances in computer methods and sensor technology. The accuracy of attitude estimates has been considerably enhanced by combining sophisticated filtering techniques like Extended Kalman Filters (EKF) with high-precision star trackers. The research demonstrates how these integrated systems improve attitude determination resilience, particularly in low Earth orbit (LEO) conditions where conventional techniques are unable to withstand increasing perturbations [17].

## 1.3 **Project Proposal**

The objective of this project is to study and develop a less complicated, cost-effective control system for launch vehicles to avoid the complexity of thrust vector control of gimbaled rocket engines using a control package that includes an aerodynamic control system (ACS) using control surfaces for endo-atmospheric control authority and a reaction control system (RCS) using small thruster for endo and exo-atmospheric control capability. This system utilizes the existing technologies that eliminate complicated rocket motors that can have actuator limits, low maneuverability, and heavy hydraulic systems. This would provide an alternative option to designing a control package for launch vehicles while providing an opportunity to develop a more powerful engine with longer burn time from the weight reduced by heavy actuators.

## 1.4 **Methodology**

To reach the established proposal, a performance analysis of an existing gimbaled launch vehicle will need to be done. Then, the study of current component space-grade components is

needed to build a simulation model of proposing a control package for launch vehicles before performing design, tune, and performance analysis to justify the proposed method. The process can be broken into parts:

*Part I: Model, simulate, and analyze the performance of an existing gimbaled rocket booster.*

- Select a current in-used launch vehicle with a gimbaled engine control package.
- Create assumptions and develop a nonlinear model from equations of motion and dynamics of the system.
- Linearize the model at different operating environments and constraints.
- Develop a model to be used in MATLAB and Simulink for six degrees of freedom simulation.
- Tune and review the performance of the baseline model.

*Part II: Provide a trade study on the components, characteristics and performance to the proposed package.*

- Perform trade study on RCS thrusters and ACS control surfaces.
- Select components for the new proposed control package based on performance, cost, and weight.

*Part III: Create the model for the new control package of the system.*

- Develop a dynamic model of the new system from the nonlinear equations.
- Linearize the simulation model with similar operating envelopes with the current, in-used model.
- In MATLAB and Simulink, develop a simulation model.
- Tune to match the performance of the baseline model.
- Perform final analysis on two systems, new and baseline judging on cost, performance …
- Conclusion and plan for future research.

# 2. Simple Inverted Pendulum

The inverted pendulum problem in Aerospace Engineering is one of the most recognizable problems in designing control systems, a classical challenge where the fundamental goal is to stabilize a pendulum that is connected to a dynamic platform, such as an airframe or spacecraft, in an upright position similar to a rocket booster. In this system, the pendulum would naturally want to return to its stable equilibrium position, which is at the angle of $270^o$ or vertically downward position, while being actively controlled to stay in its unstable equilibrium position of $90^o$ or upright and remain balanced despite the external and internal disturbances. The inverter pendulum problem is critical in the design of control systems for various aerospace applications, such as spacecraft attitude control or landing gear stabilization. Due to the nature of aerospace environments being always dynamic, the control systems must be designed to dynamically compensate for changing forces or torques applied onto the pendulum at any location to counteract the motion of the pendulum returning to its stable equilibrium position. This problem exemplifies the complex dynamics and real-time control challenges faced in Aerospace Engineering, where maintaining stability in an inherently unstable system is crucial for mission success. Therefore, it's best to analyze and design simpler control systems from a simpler model with much fewer external disturbances. There will be two different pendulum models, one with control torque authorities coming from the base, much similar to a gimbal rocket booster, with thrust vector control to direct force for attitude determination ability. On the other hand, the next model will be based on a rocket booster with no gimballed rocket engine, which is replaced with mini thrusters placed forward into the booster that can provide similar attitude control authority.

The problem of designing a control system for a rocket booster can be simplified into a model of a simple inverted pendulum, where the control authority provided to keep the pendulum is the pivot point, which outputs attitude control just like what a gimbaled rocket can do for a rocket booster. The thrust vector control ability will provide the direct torque at the base of the rocket booster, or in this case, an inverted pendulum.

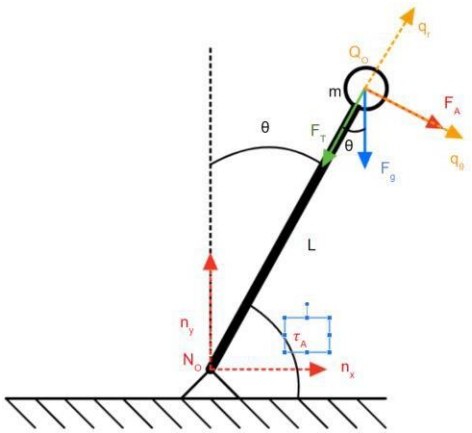


Figure 2-1 – Simplified inverted pendulum.

To begin with the problem, preliminary parameters such as assumptions are needed to avoid any possible ambiguity while proceeding forward. Since a simple inverted pendulum,

assuming a constant point mass of m [kg] placed on top of the pendulum. The pendulum rod that connected the point mass to the base is massless and has a constant length of L [m] within a frictionless environment (no friction between rod and base). The problem is considered a planar pendulum problem with a constant gravity environment, excluding air friction, drag, or resistance.

Next, analyzing the dynamic state of the system is required by deriving the governing equation of motion for the given inverted pendulum system. Since there is a torque τ [Nm] applied to the pendulum rod at the base to provide attitude control authority, a force F [N] is applied at the origin, distance L away from mass m while under the influence of gravity with gravitational acceleration g [m/s$^2$] as follows:

$$\vec{\tau}_A = {}^{N_o}(\vec{r})^{Q_o} \times \vec{F}_A \tag{2.1}$$

And,

$${}^{N_o}\boldsymbol{r}^{Q_o} = L\hat{q}_r \tag{2.2}$$

Hence continuing the Golden Rule of vector differentiation as:

$$A\frac{d}{dt}x = B\frac{d}{dt}x + {}^{A}\vec{\omega}^{B} \times x \tag{2.3}$$

Applying the Golden Rule in *(2.3)* into *(2.2)* to acquire the acceleration factor of the equation of motion as:

$${}^{N_o}\boldsymbol{v}^{Q_o} = N\frac{d}{dt}{}^{N_o}\boldsymbol{r}^{Q_o}$$

$$N\frac{d}{dt}{}^{N_o}\boldsymbol{r}^{Q_o} = Q\frac{d}{dt}{}^{N_o}\boldsymbol{r}^{Q_o} + {}^{N}\vec{\omega}^{Q} \times {}^{N_o}\boldsymbol{r}^{Q_o}$$

$$\frac{N}{dt}^{d}{}^{N_o}\boldsymbol{r}^{Q_o} = \frac{Q}{dt}^{d}(L\hat{q})_r + (\theta\hat{q})_z \times (L\hat{q})_r$$

$$\frac{N}{dt}^{d}{}^{N_o}\boldsymbol{r}^{Q_o} = \frac{Q}{dt}^{d}(-L\hat{q})_r + (\theta\hat{q})_z \times (L\hat{q})_r$$

$${}^{N_o}\boldsymbol{v}^{Q_o} = Q\frac{d}{dt}{}^{N_o}\boldsymbol{r}^{Q_o} = L\dot{\theta}\hat{q}_\theta \tag{2.4}$$

Following the rule of vector differentiation of *(2.3)* applied to *(2.4)*, the acceleration component can be found as:

$${}^{N_o}\boldsymbol{a}^{Q_o} = N\frac{d}{dt}{}^{N_o}\boldsymbol{v}^{Q_o}$$

$$\frac{N}{dt}^{d}{}^{N_o}\boldsymbol{v}^{Q_o} = \frac{Q}{dt}^{d}(L\dot{\theta}\hat{q})_\theta + {}^{N}\vec{\omega}^{Q} \times (L\dot{\theta}\hat{q})_\theta$$

$$\frac{{}^{N}d}{dt}\left({}^{N}v^{Q_o}\right) = L\ddot{\theta}\hat{q}_\theta + (\dot{\theta}\hat{q}_z) \times (L\dot{\theta}\hat{q}_\theta)$$

$${}^{N_o}a^{Q_o} = L\ddot{\theta}\hat{q}_\theta - L\dot{\theta}^2\hat{q}_r \qquad (2.5)$$

In addition, at any angle $\theta$, the point mass would constantly be under the influence of gravitation force while encountering tension force against the weight of the mass and the applied force as the input from the torque motor at the base. In which, the forces are as follows:

$$F^Q = F_T(-\hat{q}_r) + mgcos\theta(\hat{q}_r) + F_A(\hat{q}_\theta) + mgsin\theta(\hat{q}_\theta) \qquad (2.6)$$

Thus,

$$F^Q = (mgcos\theta - F_T)\hat{q}_r + (F_A - mgsin\theta)\hat{q}_\theta \qquad (2.7)$$

Therefore, apply Newton's 2nd Law of Motion to *(2.8)* as:

$$F^Q = m\,{}^{N_o}a^{Q_o} \qquad (2.8)$$

In $\hat{q}_r$, the centripetal forces and centripetal acceleration as:

$$mgcos\theta - F_T = -mL\dot{\theta}^2 \qquad (2.9)$$

And the governing equation of motion in $\hat{q}_\theta$:

$$F_A - mgsin\theta = mL\ddot{\theta} \qquad (2.10)$$

Additional analysis of *(2.10)* for:

$$\left(\frac{1}{mL}\right)F_A - \frac{g}{L}sin\theta = \ddot{\theta}$$

$$\ddot{\theta} + \frac{g}{L}sin\theta = \left(\frac{1}{mL^2}\right)F_A \cdot L$$

$$\ddot{\theta} + \frac{g}{L}sin\theta = \left(\frac{1}{mL^2}\right)\tau_A \qquad (2.11)$$

Hence if assign $\theta$ to $x_1$, $\dot{\theta}$ to $x_2$ and $\tau_A$ to u, where $\begin{bmatrix} x_1 \\ x_2 \end{bmatrix} = \begin{bmatrix} \theta \\ \dot{\theta} \end{bmatrix}$ is the state vector, and vector u is the control input vector, thus the nonlinear pendulum dynamical system linearized with small angle approximation as:

$$sinx = x \qquad (2.12)$$

Hence, the system can be represented as:

$$\begin{cases} \dot{x}_1 = x_2 \\ \dot{x}_2 = -\frac{g}{L}x_1 + \frac{1}{mL^2}u \end{cases} \quad (2.13)$$

And the open-loop linearized state-space system of the simple inverted pendulum about its unstable equilibrium point $\begin{bmatrix} x_1 \\ x_2 \end{bmatrix} = \begin{bmatrix} \pi \\ 0 \end{bmatrix}$ is:

$$\begin{bmatrix} \dot{x}_1 \\ \dot{x}_2 \end{bmatrix} = \begin{bmatrix} 0 & 1 \\ \frac{g}{L} & 0 \end{bmatrix} \begin{bmatrix} x_1 \\ x_2 \end{bmatrix} + \begin{bmatrix} 0 \\ \frac{1}{mL^2} \end{bmatrix} u \quad (2.14)$$

Meanwhile, state and output equations can be expressed as:

$$\begin{cases} \dot{x} = Ax + B\vec{u} \\ y = C\,x + D\vec{u} \end{cases} \quad (2.15)$$

Where A is the state matrix, B is the input matrix, C is the output matrix and D is the feedforward matrix. Therefore, $A = \begin{bmatrix} 0 & 1 \\ \frac{g}{L} & 0 \end{bmatrix}$, $B = \begin{bmatrix} 0 \\ \frac{1}{mL^2} \end{bmatrix}$, $C = [1 \quad 0]$ since the only interested output is the attitude angle $\theta$, and no feedforward matrix. From *(2.13)*, the transfer function of the open-loop system can be done via Lagrange transform on both sides of the equal sign as:

$$\mathcal{L}(\ddot{\theta}) = \mathcal{L}\left[\frac{g}{L}\theta + \frac{1}{mL^2}u(s)\right]$$

$$s^2\theta(s) = \frac{g}{L}\theta(s) + \frac{1}{mL^2}u(s)$$

$$\frac{\theta(s)}{u(s)} = \frac{\frac{1}{mL^2}}{s^2 - \frac{g}{L}} \quad (2.16)$$

First, the closed-loop model is designed using an LQR controller with controller gain K, state matrix A, input matrix B, and controller matrices Q, and R. Since there is only one input of keeping the pendulum put right at $\theta = 0^o$ and 2 state attitude angle and angle rate; R and Q are the diagonals of 1x1 and 2x2 matrices. A closed-loop simulation model can be created using an LQR controller to reject external disturbances as follows:

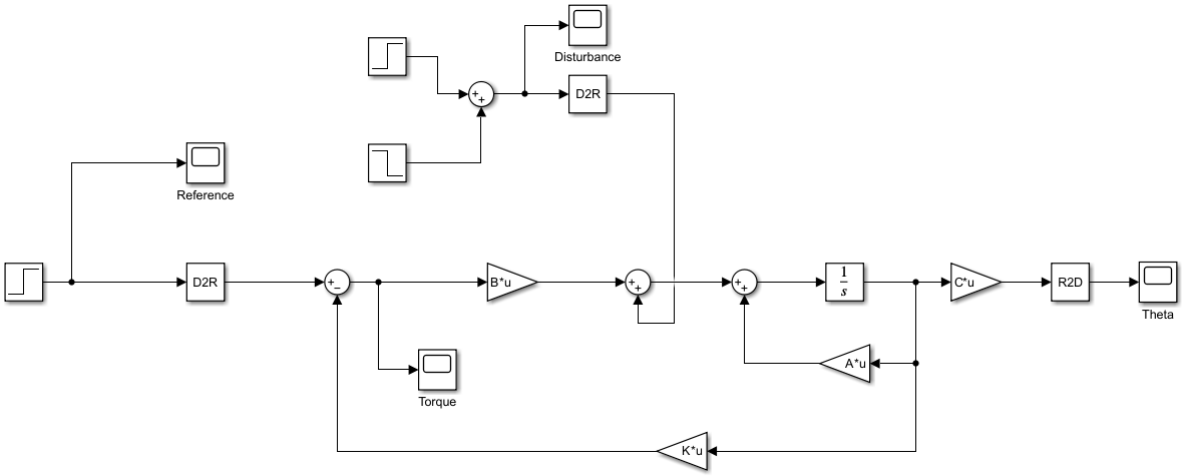


Figure 2-2 – Closed-loop Simulink model of simple inverted pendulum with controller LQR for external disturbance rejection.

As the system shown in Figure 2-2, it can be seen in Figure 2-3 that due to a high-cost function J, where J is:

$$J = \int_0^\infty (x^T Q x + u^T R u) dt \qquad (2.17)$$

The response of the system is fairly quick with the cost of Q and R.

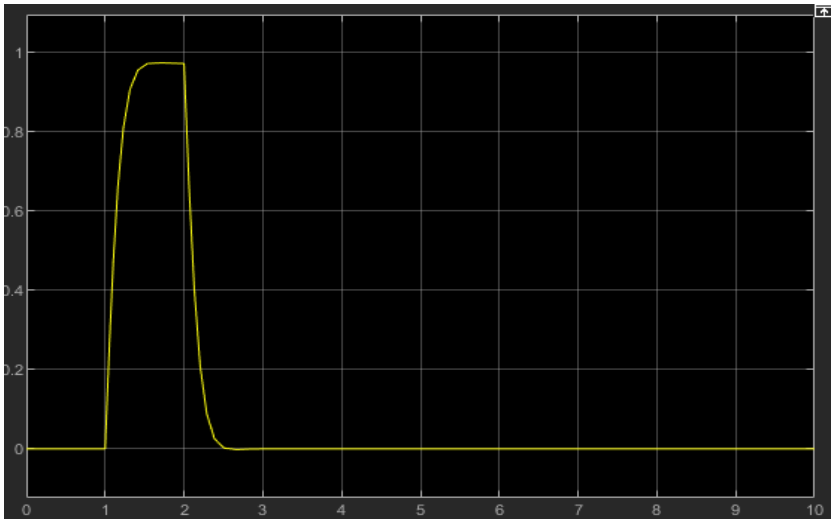


Figure 2-3 – Attitude angle $\theta$ in response to disturbance using the LQR controller

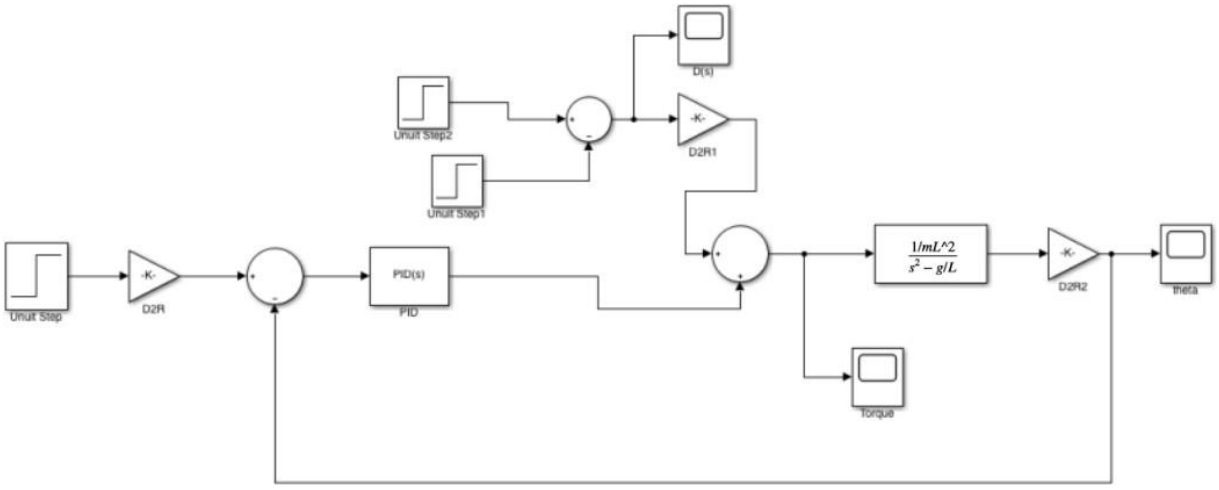


Figure 2-4 – Closed-loop Simulink model of simple inverted pendulum with PID controller for external disturbance.

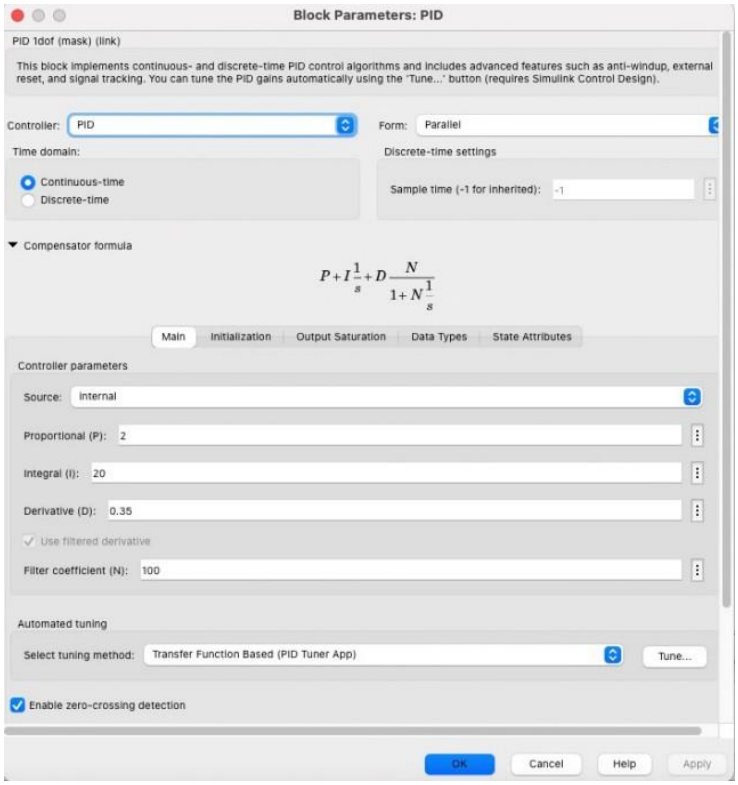


Figure 2-5 – PID tuning specification

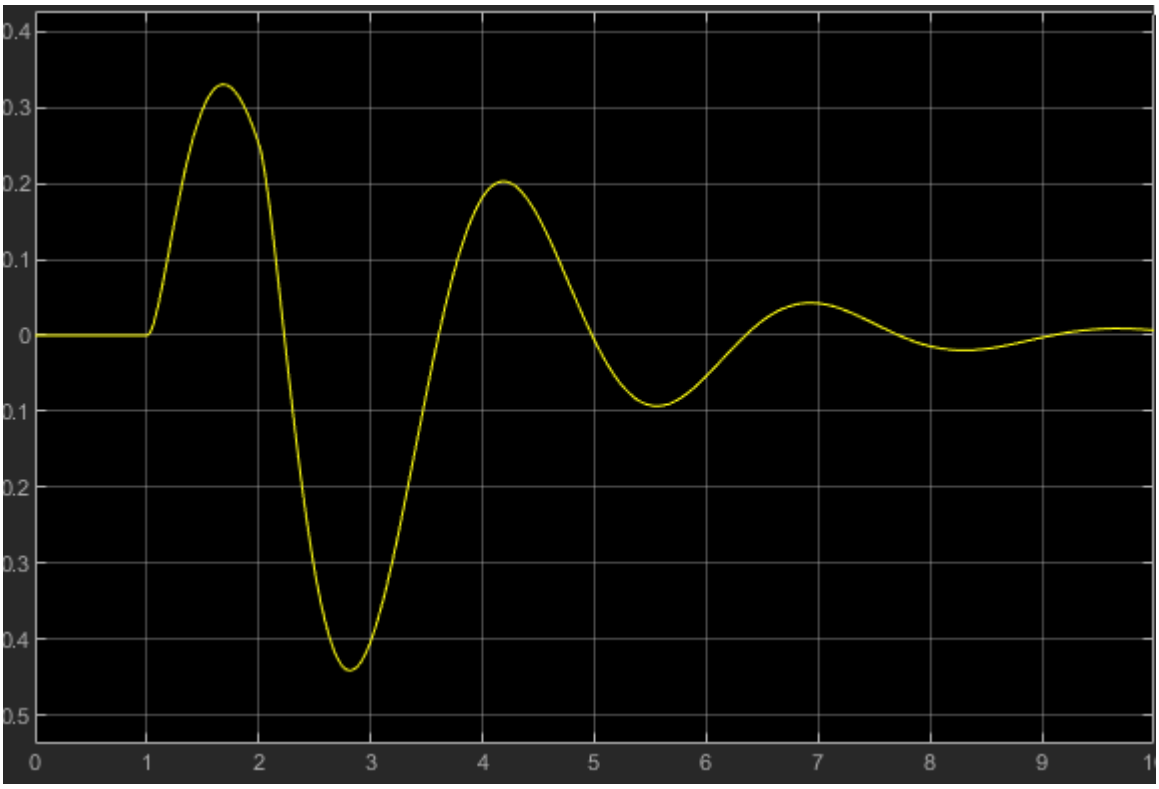

Figure 2-6 – Attitude angle $\theta$ in response to disturbance using the LQR controller

Due to the blend of PID, it can be seen that even with low P value, the system still overshoots the reference signal by quite a margin. However, with the blend of I and D controller gain, it can be seen that the system is trying to correct steady-state error while quickly damp out the oscillation.

# 3. Inverted Pendulum on Rolling Cart

In the same process as for the simple inverted pendulum model, the inverted pendulum on the cart has a similar setup with the exception of having a controllable cart that can move in a 2-dimensional plane and acts as a torque motor to provide attitude control to allow the pendulum to stay upright instead of a fixed base pendulum with a torque motor at base. This simulation model offers higher levels of fidelity than the previous one. For this system, the control input is a force modeling thrust vectoring that moves the cart horizontally allowing the outputs of the angular position of the pendulum, modeling pitch/yaw angle and horizontal position of the cart modeling 3 degrees of freedom of the rocket.

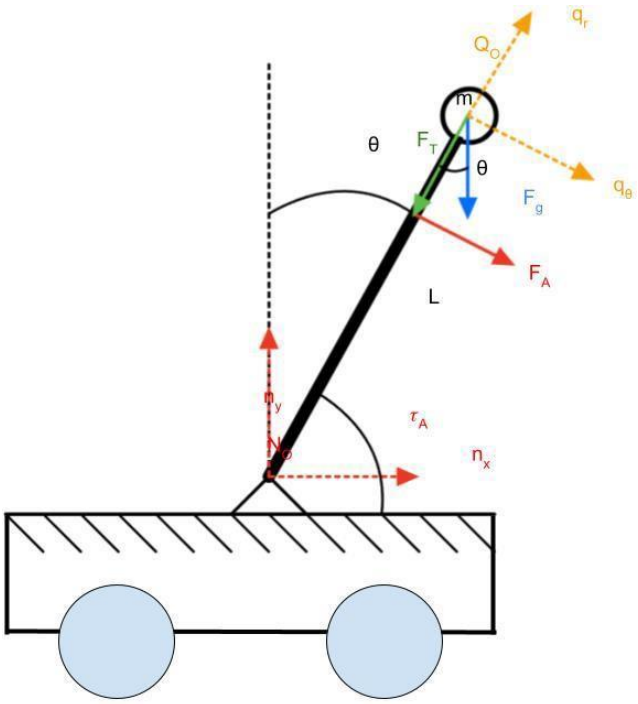


Figure 3-1 The inverted pendulum on a cart

In the same fashion, in order to analyze the simulation model and turn its control systems, assumptions must be made to allow the simulation model to operate within the intended boundaries. Despite being a higher level of fidelity model than the simple inverted pendulum, this is still a quite simplified model, with both moving parts in the cart and the inverted are uniform point mass objects including a point mass sphere of mass m [kg] placing on top of a massless pendulum rod, with length L [m] that stands on a mass cart M [kg] which can move horizontally . At the same time, all objects are bound within a frictionless environment, with no friction between the pendulum rod and the cart, between the wheels and the cart's mainframe, or

the wheels with the surface. The problem is also considered a planar pendulum problem with a constant gravity environment, excluding air friction, drag, or resistance.

Next, analyzing the dynamic state of the system is required by deriving the governing equations of motion for the given inverted pendulum system. The attitude position of the pendulum $\theta$ is controlled by providing an applied force F [N] onto the cart on the horizontal plan x [m] while under the influence of gravity with gravitational acceleration g [m/s$^2$].

Beginning with the cart, analyzing the free-body diagram of the cart for the combination of forces, the equation of motion is as follows:

$$\vec{F}^{C}_{A} + \vec{F}^{C}_{R} + \vec{F}_{N} + \vec{F}^{C}_{g} = M\,a \tag{3.1}$$

Where $\vec{F}^{C}_{R}$ is the reaction force from the pendulum onto the cart, $\vec{F}^{C}_{A}$ is the applied force onto the cart to assist attitude control for the pendulum, $\vec{F}_{N}$ is the normal force of the ground onto the cart and $\vec{F}^{C}_{A}$ is the gravitational force applied to the cart while $\ddot{x}$ is the acceleration of the cart. However, only forces in the x-direction would have a meaningful impact on the cart's acceleration. In addition, to make it easier moving forward, the reaction $\vec{F}^{C}_{R}$ will be written as $F^{C}_{x}$ and $F^{C}_{y}$ when broken down into components for the x-axis and the y-axis, hence, *(3.1)* is rewritten to isolate the forces in the x-plane of the system as follows:

$$\vec{i}^{\,C}_{A} + \vec{i}^{\,C}_{R} = M\,a \tag{3.2}$$

Or as,

$$F^{C}_{A} + F^{C}_{x} = M\ddot{x} \tag{3.3}$$

Where $\ddot{x}$ represents the acceleration the cart would experience under the combined forces in the x-direction. Next, the second element of the system, summing up the net forces applying to the inverted pendulum as follows:

$$\vec{F}^{P}_{R} + \vec{F}^{P}_{g} = m\vec{\ddot{a}}_{P} \tag{3.4}$$

Noticing in *(3.2)* and *(3.4)*, the cart and the pendulum would be experiencing different accelerations, $a$ and $\vec{\ddot{a}}_{P}$. Now in a similar fashion, isolating the y-direction and x-direction forces as follows:

$$F^{P}_{y} - F^{P}_{g} = m\ddot{y}_{P} \tag{3.5}$$

And,

$$F^{P}_{x} = m\ddot{x}_{P} \tag{3.6}$$

Where $\vec{F}^{P}_{R}$ is the reaction force of the cart onto the pendulum. Similar to $\vec{F}^{C}_{R}$, $\vec{F}^{C}_{R}$ will also be broken down into $F^{P}_{x}$ while referring to the x component of the reaction force from the cart onto the pendulum $F^{P}_{y}$ while referencing the y component of the reaction force. Now to unify *(3.5)* and *(3.6)*, the acceleration the pendulum would experience can be addressed in an equation of the cart's acceleration as follows:

$$x_p = x + Lsin\theta \tag{3.7}$$

Taking the derivative of *(3.7)* with respect to time:

$$\dot{x_P} = \dot{x} + L\theta cos\theta \tag{3.8}$$

To achieve the pendulum's acceleration, take the derivative of *(3.8)* with respect to time as follows:

$$\ddot{x_P} = \ddot{x} + L\ddot{\theta}cos\theta - L\dot{\theta^2}\ sin\theta \tag{3.9}$$

In a similar fashion, $y_p$ can be derived as:

$$y_p = Lcos\theta \tag{3.10}$$

Taking the derivative of *(3.10)* with respect to time:

$$\dot{y_P} = -L\theta sin\theta \tag{3.11}$$

To achieve the pendulum's acceleration, take the derivative of *(3.8)* with respect to time as follows:

$$\ddot{y_P} = -L\ddot{\theta}sin\theta + L\dot{\theta^2}\ cos\theta \tag{3.12}$$

Now substitute *(3.9)* and into *(3.6)* for:

$$F^{P}_{x} = m\ddot{x} + mL\ddot{\theta}cos\theta - mL\dot{\theta^2}\ sin\theta \tag{3.13}$$

According to Newton's third law of motion, when two objects interact, they apply forces of equal magnitude and opposite directions to each other. Hence, the reaction forces of the cart and the pendulum onto each other are equal:

$$F^{P}_{x} = -F^{C}_{x} \tag{3.14}$$

Combining *(3.11)* and *(3.3)* results in the first equation of motion for the overall system of an inverted pendulum on a cart as follows:

$$F^{C}_{A} - m\ddot{x} - mL\ddot{\theta}cos\theta + mL\dot{\theta^2}\ sin\theta = M\ddot{x}$$

$$F^{C}_{A} = M\ddot{x} + m\ddot{x} + mL\ddot{\theta}cos\theta - mL\dot{\theta^2}\ sin\theta$$

$$F^{C}_{A} = (M + m)\ddot{x} + mL(\ddot{\theta}cos\theta - \dot{\theta^2}\ sin\theta) \quad (3.15)$$

Due to this being non-linearized, the dynamical system can be linearized with small angle approximation in *(2.15)* with the assumption that controlled angle $\theta$ would only stay in a small neighborhood of around $0^o$ as that is the goal of the system, is to keep the pendulum vertically upright at an angle of $90^o$.

$$cosx \approx 1 \quad (3.16)$$

And,

$$\dot{\theta^2}\ \approx 0 \quad (3.17)$$

Hence if assign $F^{C}_{A}$ to u as the control input vector, and the first 3 stages of the state vector is $[\theta\ \dot{\theta}\ \ddot{x}]$. Thus, the nonlinear pendulum dynamical system linearized with small angle approximation as:

$$(M + m)\ddot{x} + mL\ddot{\theta} = u \quad (3.18)$$

Let's take a look at the forces applied on the pendulum in the y-direction from *(3.5)* as the pendulum is under the influence of the reaction force from the cart and the gravitational force and substitute the y-direction acceleration acquired from *(3.12)* as follows:

$$F^{P}_{y} - F^{P}_{g} = m(-L\ddot{\theta}sin\theta + L\dot{\theta^2}\ cos\theta)$$

$$F^{P}_{y} - mg = m(-L\ddot{\theta}sin\theta + L\dot{\theta^2}\ cos\theta) \quad (3.19)$$

As specified before, $F^{P}_{x}$ and $F^{P}_{y}$ are the horizontal and vertical components of the reaction applied on the pendulum from the rolling cart. Therefore, they can be derived as the function of the reaction force as follows:

$$F^{P}_{x}\hat{\imath} = \vec{F^{P}}_{R}sin\theta \quad (3.20)$$

With the magnitude of:

$$F^{P}_{x} = |\vec{F^{P}}_{R}|sin\theta \quad (3.21)$$

And,

$$F^{P}_{y}\hat{\jmath} = \vec{F^{P}}_{R}cos\theta \quad (3.22)$$

Magnitude of:

$$F^P{}_y = |\overrightarrow{\overrightarrow{F}^P}_R| cos\theta \quad (3.23)$$

Now, substitute $F^P{}_x$ acquired from *(3.21)* into *(3.11)*, and $F^P{}_y$ acquired from *(3.23)* into *(3.13)* to get:

$$|\overrightarrow{\overrightarrow{F}^P}_R| sin\theta = m\ddot{x} + mL\ddot{\theta} cos\theta - mL\dot{\theta}^2 \, sin\theta \quad (3.22)$$

And,

$$|\overrightarrow{\overrightarrow{F}^P}_R| \, cos\theta - mg = m(-L\ddot{\theta} sin\theta - L\dot{\theta}^2 \, cos\theta) \quad (3.23)$$

Now, multiply $cos\theta$ to *(3.22)* and $sin\theta$ to *(3.23)* for the next step:

$$|\overrightarrow{\overrightarrow{F}^P}_R| sin\theta cos\theta = m\ddot{x} cos\theta + mL\ddot{\theta}(cos\theta)^2 - mL\dot{\theta}^2 \, sin\theta cos\theta \quad (3.24)$$

And,

$$|\overrightarrow{\overrightarrow{F}^P}_R| \, cos\theta sin\theta - mgsin\theta = -mL\dot{\theta}^2 \, cos\theta sin\theta - mL\ddot{\theta}(sin\theta)^2 \quad (3.25)$$

Subtract *(3.25)* from *(3.24)* for the left-hand side:

$$|\overrightarrow{\overrightarrow{F}^P}_R| \, sin\theta cos\theta - |\overrightarrow{\overrightarrow{F}^P}_R| \, cos\theta sin\theta + mgsin\theta$$

$$mgsin\theta \quad (3.26)$$

The right-hand side of the equation is:

$$m\ddot{x} cos\theta + mL\ddot{\theta}(cos\theta)^2 - mL\dot{\theta}^2 \, sin\theta cos\theta + mL\dot{\theta}^2 \, cos\theta sin\theta + mL\ddot{\theta}(sin\theta)^2$$

$$m\ddot{x} cos\theta + mL\ddot{\theta} \quad (3.27)$$

Therefore, as the result of combining the left-hand side and the right-hand side of the equation as follows:

$$mgsin\theta = m\ddot{x} cos\theta + mL\ddot{\theta} \quad (3.28)$$

Similarly, linearized *(3.28)* in the same process with *(2.13)*, *(3.16)*, and *(3.17)* as in *(3.18)* to result:

$$mg\theta = m\ddot{x} + mL\ddot{\theta} \quad (3.29)$$

Or,

$$g\theta = \ddot{x} + L\ddot{\theta} \quad (3.30)$$

Now, with *(3.30)*, the second governing equation of motion for the system is introduced. However, it must be pointed out that, *(3.30)* is only qualified as the second governing equation for the system due to the fact that this simulation model uses a uniform point mass sphere placed on top of a massless inverted pendulum. Hence all the mass is not uniformly distributed but is concentrated in the top end of the pendulum. Therefore, it is possible to ignore the moment of inertia that then would possibly exist on a uniformly distributed pendulum rod rotating about it fixed point at the lower end of the rod. A scenario where the pendulum is a uniformly distributed rod would also be derived below to show the comparison between two different condition setups for the differences.

Now the overall system can be represented as:

$$\begin{cases} (M+m)\ddot{x} + mL\ddot{\theta} = u \\ g\theta = \ddot{x} + L\ddot{\theta} \end{cases} \tag{3.31}$$

However, *(3.31)* contains two equations that are coupled together. Therefore, it would be necessary to further decouple them, and now return to (*3.29)*, before simplifying mass m [kg] out of the equation to achieve *(3.30)*, by isolating $mL\ddot{\theta}$ in (*3.18)* and *(3.29)* for:

$$\begin{cases} mL\ddot{\theta} = u - (M+m)\ddot{x} \\ mL\ddot{\theta} = m\ddot{x} - mg\theta \end{cases} \tag{3.32}$$

Therefore, *(3.32)* would result in the first decoupled governing equation of motion for the system as:

$$u - (M+m)\ddot{x} = m\ddot{x} - mg\theta$$

$$M\ddot{x} = u - mg\theta \tag{3.33}$$

In a similar fashion to *(3.33)*, to decouple *(3.18)*, isolating the term $\ddot{x}$ in (*3.30)* to create a similar equation as:

$$\ddot{x} = L\ddot{\theta} - g\theta \tag{3.34}$$

Now substituting *(3.34)* into *(3.18)* to acquire the other decoupled governing equation of motion of the system as follows:

$$(M+m)(L\ddot{\theta} - g\theta) + mL\ddot{\theta} = u$$

$$mL\ddot{\theta} = (M+m)g\theta - u \tag{3.35}$$

Hence, the simulation model of the system with the second order, linearized and decoupled is as follows:

$$\begin{cases} M\ddot{x} = -mg\theta + u \\ mL\theta = (M+m)g\theta - u \end{cases} \quad (3.36)$$

Isolating $\ddot{x}$ and $\theta$ for:

$$\begin{cases} \ddot{x} = \frac{-mg}{M}\theta + \frac{1}{M}u \\ \theta = \frac{(M+m)g}{mL}\theta - \frac{1}{mL}u \end{cases} \quad (3.37)$$

Let $x$ be $x_1$, $\dot{x}$ be $x_2$ or $\dot{x}_1$, then $\ddot{x}$ would be $\dot{x}_2$, and $\theta$ be $x_3$, $\theta$ be $x_4$ or $\dot{x}_3$, then $\theta$ would be $\dot{x}_4$, where $\begin{bmatrix} x_1 \\ x_2 \\ x_3 \\ x_4 \end{bmatrix} = \begin{bmatrix} x \\ \dot{x} \\ \theta \\ \theta \end{bmatrix}$ is the state vector, and vector u is the control input vector.
Therefore, the open-loop linearized state-space system of the inverted pendulum about its unstable equilibrium point is:

$$\begin{bmatrix} \dot{x}_1 \\ \dot{x}_2 \\ \dot{x}_3 \\ \dot{x}_4 \end{bmatrix} = \begin{bmatrix} 0 & 1 & 0 & 0 \\ 0 & 0 & \frac{-mg}{M} & 0 \\ 0 & 0 & 0 & 1 \\ 0 & 0 & \frac{(m+M)g}{mL} & 0 \end{bmatrix} \begin{bmatrix} x_1 \\ x_2 \\ x_3 \\ x_4 \end{bmatrix} + \begin{bmatrix} 0 \\ \frac{1}{M} \\ 0 \\ -\frac{1}{mL} \end{bmatrix} u \quad (3.38)$$

Meanwhile, state and output equations can be expressed as:

$$\begin{cases} \dot{x} = Ax + B\vec{u} \\ y = C\,x + D\vec{u} \end{cases} \quad (3.39)$$

Where A is the state matrix, B is the input matrix, C is the output matrix and D is the feedforward matrix. Therefore, $A = \begin{bmatrix} 0 & 1 & 0 & 0 \\ 0 & 0 & \frac{-mg}{M} & 0 \\ 0 & 0 & 0 & 1 \\ 0 & 0 & \frac{(m+M)g}{mL} & 0 \end{bmatrix}$, $B = \begin{bmatrix} 0 \\ \frac{1}{M} \\ 0 \\ -\frac{1}{mL} \end{bmatrix}$, $C = [0 \quad 0 \quad 1 \quad 0]$, since the only interested output is the attitude angle y = $\theta$, and no feedforward matrix. From *(3.37)*, the transfer function of the open-loop system can be done via the Lagrange transform on both sides of the equal sign as:

$$\mathcal{L}(\theta) = \mathcal{L}\left[\frac{(M+m)g}{mL}\theta - \frac{1}{mL}u(s)\right]$$

$$s^2\theta(s) = \frac{(M+m)g}{mL}\theta(s) - \frac{1}{mL}u(s)$$

$$\frac{\theta(s)}{u(s)} = \frac{-\frac{1}{mL}}{s^2 - \frac{(M+m)g}{mL}} \qquad (3.40)$$

Checking the controllability of the system with the controllability matrix Co can be defined as:

$$Co = [B \quad AB \quad A^2B \quad \cdots \quad A^{(n-1)}B] \qquad (3.41)$$

Where A is still the state matrix while B is still the input matrix, and "n" is the number of states, in this particular system, n is 4. Therefore, the controllability matrix can be achieved from *(3.41)* as follows:

$$Co = [B \quad AB \quad A^2B \quad A^3B] \qquad (3.41)$$

Calculating the components of the controllability matrix, $AB$:

$$AB = \begin{bmatrix} 0 & 1 & 0 & 0 \\ 0 & 0 & \frac{-mg}{M} & 0 \\ 0 & 0 & 0 & 1 \\ 0 & 0 & \frac{(m+M)g}{mL} & 0 \end{bmatrix} \begin{bmatrix} 0 \\ \frac{1}{M} \\ 0 \\ -\frac{1}{mL} \end{bmatrix} = \begin{bmatrix} \frac{-mg}{M} \\ 0 \\ 0 \\ 0 \end{bmatrix} \qquad (3.42)$$

Calculating $A^2B$:

$$A^2B = \begin{bmatrix} 0 & 1 & 0 & 0 \\ 0 & 0 & \frac{-mg}{M} & 0 \\ 0 & 0 & 0 & 1 \\ 0 & 0 & \frac{(m+M)g}{mL} & 0 \end{bmatrix}^2 \begin{bmatrix} 0 \\ \frac{1}{M} \\ 0 \\ -\frac{1}{mL} \end{bmatrix} = \begin{bmatrix} 0 \\ \frac{g}{ML} \\ 0 \\ \frac{-(m+M)g}{(mL)^2} \end{bmatrix} \qquad (3.43)$$

Calculating $A^3B$:

$$A^3B = \begin{bmatrix} 0 & 1 & 0 & 0 \\ 0 & 0 & \frac{-mg}{M} & 0 \\ 0 & 0 & 0 & 1 \\ 0 & 0 & \frac{(m+M)g}{mL} & 0 \end{bmatrix}^3 \begin{bmatrix} 0 \\ \frac{1}{M} \\ 0 \\ -\frac{1}{mL} \end{bmatrix} = \begin{bmatrix} \frac{g}{ML} \\ 0 \\ \frac{-(m+M)g}{(mL)^2} \\ 0 \end{bmatrix} \qquad (3.44)$$

$$Co = \begin{bmatrix} 0 & \frac{-mg}{M} & 0 & \frac{g}{ML} \\ \frac{1}{M} & 0 & \frac{g}{ML} & 0 \\ 0 & 0 & 0 & \frac{-(m+M)g}{(mL)^2} \\ -\frac{1}{mL} & 0 & \frac{-(m+M)g}{(mL)^2} & 0 \end{bmatrix} \quad (3.45)$$

Now, to determine whether the system is fully controllable or not via taking the Rank of the controllability matrix, resulting in:

$$Rank(Co) = 4 \quad (3.46)$$

The system is fully controllable as it is full rank. In addition, this can also be determined by observing the presence of input control vector u in both governing equations of motion of the system.

To simulate the model, parameters need to be assigned for the cart's mass. M = 3 [kg], the mass of the sphere located on top of the inverted pendulum, m = 1 [kg], the length of the massless inverted pendulum, L = 1 [m], while gravitational acceleration is g = 9.81 [kg/s$^2$]. For initializing the system with the initial conditions of $x_i = \begin{bmatrix} x_1 \\ x_2 \\ x_3 \\ x_4 \end{bmatrix} = \begin{bmatrix} x \\ \dot{x} \\ \theta \\ \dot{\theta} \end{bmatrix} = \begin{bmatrix} 0 \\ 0 \\ 0.01 \\ 0 \end{bmatrix}$, where the cart would start at the origin, with no velocity, while the pendulum is set to be slightly off-set to the equilibrium of 0-degree angle and has no angular velocity.

Now, with the initial position given as the starting state of the system, the desired state of the system can be $x_f = \begin{bmatrix} x_1 \\ x_2 \\ x_3 \\ x_4 \end{bmatrix} = \begin{bmatrix} x \\ \dot{x} \\ \theta \\ \dot{\theta} \end{bmatrix} = \begin{bmatrix} 1 \\ 0 \\ 0 \\ 0 \end{bmatrix}$, where the final position is an arbitrary location away from the origin, in this case, is 1, while not translational and angular velocity residue is wanted and the inverted pendulum to stay fully upward at an angle $\theta = 0$.

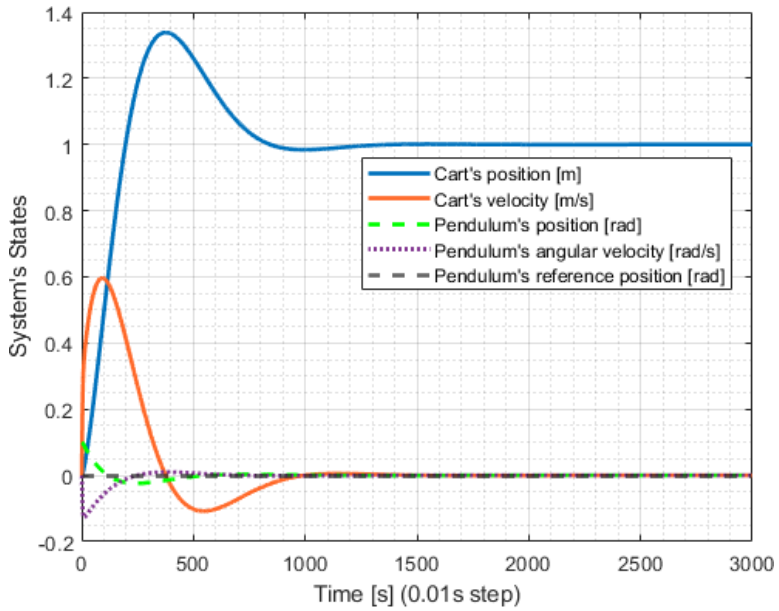


Figure 3-2 The system's Closed-Loop Response with $\theta_4$ = 0.1

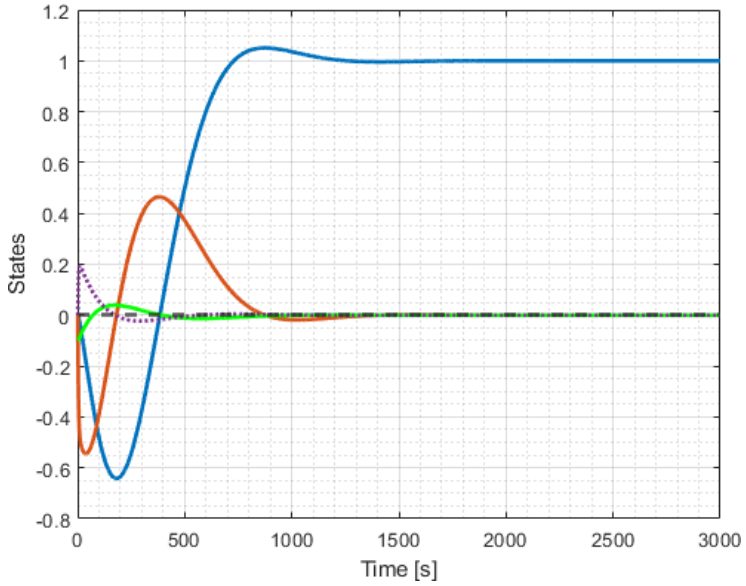


Figure 3-3 The system's Closed-Loop Response with $\theta_4$ = -0.1

Notice that the time step in the simulation is at 0.001, hence the simulation time reflected in the result is taking almost 3000 steps or 30 seconds to reach the reference or desired states of the system. It is worth noticing that despite having a relatively small R-value for the cost function J, the emphasis is placed heavily on the error of $x_3$ and $x_4$, which in this case are $\theta$ and $\theta$ from matrix Q (see Appendix A), where R would be the cost to the input from the hardware while Q is the "cost" accounting for the system's states and how each state is weighted. The cost function of a Linear Quadratic Regulator can be calculated as:

$$J = \int_0^\infty (x^T Q x + u^T R u) dt \qquad (3.47)$$

Via data analysis, it can be seen that in case 1 $\theta_4$ = 0.1, Figure 3-2, the cart accelerates quickly in the positive direction to cause an impulse to the pendulum via reaction force between the cart and the inverted pendulum which causes the cart to massively overshoot its desired steady-state position. On the other hand, where $\theta_4$ = -0.1, like in Figure 3-3, the system started moving left in the negative direction initially, which is the wrong direction as the reference position is x = 1. This behavior is seen by the system only caused by the initial position of the pendulum, which reflects that the overall system is a *non-minimum phase*. This is similar to putting a thermostat into a hot cup of water, the reading would go down for a quick moment before going up.

However, in many cases, there would be disturbances and noise within the system due to multiple factors such as the lack of sensors to measure many states or any possible noisy sensor measurements. Now, these factors can be mitigated via filtering, a prime example can be the Kalman filter, the most important and popular state estimator of uncertain information of a dynamical system based on the knowledge of any possible disturbances, after developing a working Kalman filter with a Linear Quadratic Regulator for better control of an unstable inverted pendulum on a cart.

Firstly, in order to acknowledge any states of the system, there must be sensors, and the system must be observable. To check whether the system is fully observable, an observable matrix can be calculated as:

$$Ob = \begin{matrix} C \\ CA \\ CA^2 \\ \vdots \\ [CA^{(n-1)}] \end{matrix} \qquad (3.48)$$

Where A is still the state matrix, , A = $\begin{matrix} 0 & 1 & 0 & 0 \\ 0 & 0 & \frac{-mg}{M} & 0 \\ 0 & 0 & 0 & 1 \\ 0 & 0 & \frac{(m+M)g}{mL} & 0 \end{matrix}$ while C is still the output matrix, C = $[0 \quad 0 \quad 1 \quad 0]$, and "n" is the number of states, in this particular system, n is 4. Therefore, the controllability matrix can be achieved from *(3.48)* as follows:

$$Ob = \begin{bmatrix} C \\ CA \\ CA^2 \\ CA^3 \end{bmatrix} \qquad (3.49)$$

Calculating the components of the observability matrix, $CA$:

$$CA = [0 \quad 0 \quad 1 \quad 0] \begin{bmatrix} 0 & 1 & 0 & 0 \\ 0 & 0 & \frac{-mg}{M} & 0 \\ 0 & 0 & 0 & 1 \\ 0 & 0 & \frac{(m+M)g}{mL} & 0 \end{bmatrix} = [0 \quad 0 \quad 0 \quad 1] \tag{3.50}$$

Calculating $A^2B$:

$$CA^2 = [0 \quad 0 \quad 1 \quad 0] \begin{bmatrix} 0 & 1 & 0 & 0 \\ 0 & 0 & \frac{-mg}{M} & 0 \\ 0 & 0 & 0 & 1 \\ 0 & 0 & \frac{(m+M)g}{mL} & 0 \end{bmatrix}^2 = [0 \quad 0 \quad \frac{(m+M)g}{mL} \quad 0] \tag{3.51}$$

Calculating $A^3B$:

$$CA^3 = [0 \quad 0 \quad 1 \quad 0] \begin{bmatrix} 0 & 1 & 0 & 0 \\ 0 & 0 & \frac{-mg}{M} & 0 \\ 0 & 0 & 0 & 1 \\ 0 & 0 & \frac{(m+M)g}{mL} & 0 \end{bmatrix}^3 = [0 \quad 0 \quad 0 \quad \frac{(m+M)g}{mL}] \tag{3.52}$$

$$Ob = \begin{bmatrix} 0 & 0 & 1 & 0 \\ 0 & 0 & 0 & 1 \\ 0 & 0 & \frac{(m+M)g}{mL} & 0 \\ 0 & 0 & 0 & \frac{(m+M)g}{mL} \end{bmatrix} \tag{3.53}$$

Now, to determine whether the system is fully controllable or not via taking the Rank of the observability matrix, resulting in:

$$Rank(Ob) = 2 \tag{3.54}$$

The system does not have full rank; therefore, it is not fully observable. Which is the case due to

However, if matrix C = $[1 \quad 0 \quad 0 \quad 0]$ instead, the rank of the observability matrix, Rank(Ob) would be 4, the system would be fully observable as it is full rank. This is the case due to sensor placement, where if the sensor is used to measure $x_3$, the pendulum's angular position, the system is not fully observable, while if the sensor is used to measure $x_1$, the position of the cart, the system is deemed to be full rank; however, due to $x_1$ does not appear explicitly in the equations of motion of the dynamical system, it is not possible to observe all other states of the system via $x_1$.

This work is not related to previous work, but more of an expansive addition to the model depending on the design of the problem.

However, if the pendulum has a uniform mass in addition to the sphere, *(3.29)* is not particularly the wanted equation of motion since it introduces another state of the pendulum that is still coupled to two existing states and missing another state for the cart. Hence, it is deemed not useful for further analysis. Therefore, to acquire the wanted equation of motion, the analysis of the sum of forces applied to the x-axis of the pendulum's frame:

$$F^{P}_{x}cos\theta - F^{P}_{y}sin\theta + mgsin\theta = m(L\ddot{\theta}) \qquad (3.55)$$

Unlike the simple inverted pendulum model in Chapter 2, the pendulum in the pendulum on a rolling cart simulation model would experience the additional acceleration term as the result of the externally applied force onto the cart of $\ddot{x}$. Hence the additional term to *(3.30)* results in:

$$F^{P}_{x}cos\theta - F^{P}_{y}sin + mgsin\theta = m(L\ddot{\theta} + \ddot{x}cos\theta) \qquad (3.56)$$

Now applying Newton's second law of rotation to the pendulum:

$$\vec{\tau}^{C}_{R} + \vec{\tau}_{g} = I\ddot{\theta} \qquad (3.57)$$

The pivot would be at the center of mass of the rod instead of at the base of the pendulum where it is connected to the cart to provide a meaningful torque to control its attitude. Hence, the torque due to gravitational force is zero while the torque from reaction force against the cart would be an axial force applied at the base with direction toward the center of mass, resulting in the torque having 2 components, following *(2.1)* to have:

$$F^{P}_{x}Lcos\theta - F^{P}_{y}Lsin\theta = -I\ddot{\theta}$$

$$F^{C}_{x}cos\theta - F^{C}_{y}sin\theta = \frac{I\ddot{\theta}}{L} \qquad (3.58)$$

To process forward, combine *(3.31)* and *(3.33)* to result in:

$$-mgLsin\theta = -I\ddot{\theta} - mL(L\ddot{\theta} + \ddot{x}cos\theta)$$

$$\ddot{x}mLcos\theta = mgLsin\theta - (I + mL^2)\ddot{\theta} \qquad (3.59)$$

Linearizing *(3.34)* in a similar fashion done previously for the second equation of motion of the system as follows:

$$\ddot{x}mL = mgL\theta - (I + mL^2)\ddot{\theta} \qquad (3.60)$$

# 4. Hardware selection

In order to create a simulation model for the proposed solution, there must be requirements for vehicle design. Therefore, this section would serve the purpose of selecting hardware for the simulation model at the low level of control system engineering rather than for the overall design and the system engineering approach. Hence, selected hardware would be only weighted based on mass, length, and max performance to create a more realistic simulation model. Based on a typical Falcon 9 launch, based on SpaceX's overview data of a Falcon 9 can be as

Table 4-1 – SpaceX's Falcon 9 specs and payload capacity [18]

| **Height (with fairing) (m)** | **Diameter (m)** | **Mass (without payload) (kg)** | **Payload to LEO (kg)** | **Payload to GTO (kg)** | **Payload to Mars (kg)** |
|---|---|---|---|---|---|
| 70 | 3.7 | 549,054 | 22,800 | 8,300 | 4,020 |

Table 4-2 – Available rocket engines [18], [19]

| **Company** | **Engine** | **Burn time (Vacuum) (s)** | **Mass (kg)** | **Thrust at sea level (kN)** | **Thrust in vacuum (kN)** |
|---|---|---|---|---|---|
| SpaceX | Merlin 1D | 397 (vacuum)<br>162 (sea level) | 1760 kg | 845 | 981 |
| Blue Origin | BE-3PM | 141 | NA | 490 | 770 |
| Blue Origin | BE-3U | N/A | N/A | N/A | 712 |
| Blue Origin | BE-7 | N/A | N/A | N/A | 44.5 |
| Aerojet Rocketdyne | RS-25 | 480 | 3,177 | 1852 | 2278 |

Table 4-3 – Reaction Control System (RCS) and Attitude Control Thrusters [20]

| **Company** | **Model** | **Isp (s)** | **Thrust range (N)** | **Mass (kg)** |
|---|---|---|---|---|
| Marotta | CGMT | N/A | 0.1 – 10 N | 0.60 |
| Aerojet Rocketdyne | MR-401 | 184 – 180 | 0.07 – 0.09 | 0.60 |
| Aerojet Rocketdyne | MR-103G | 224 – 202 | 0.19 – 1.13 | 0.33 |
| Aerojet Rocketdyne | MR-103J | 229 – 219 | 0.19 – 1.13 | 0.37 |
| Aerojet Rocketdyne | MR-111G | 229 – 219 | 1.8 – 4.9 | 0.37 |
| Aerojet Rocketdyne | MR-106L | 235 – 228 | 4 – 10 | 0.59 |
| Aerojet Rocketdyne | MR-107T | 225 – 222 | 54 – 125 | 1.01 |
| Aerojet Rocketdyne | MR-107S | 236 – 225 | 85 – 360 | 1.01 |
| Aerojet Rocketdyne | MR-107U | 229 – 223 | 182 – 307 | 1.38 |
| Aerojet Rocketdyne | MR-107V | 229 – 223 | 67 – 220 | 1.01 |
| Aerojet Rocketdyne | MR-104H | 237 – 22 | 201 – 554.2 | 2.40 |
| Aerojet Rocketdyne | MR-104J | 223 – 215 | 440 – 614 | 6.44 |
| Aerojet Rocketdyne | MR-80B | 225 – 200 | 31 – 3630 | 168 |

Table 4-4 – Commercially available reaction wheels and specs [25].

| **Company** | **Model** | **Momentum (Nms)** | **Mass (kg)** | **Volume (mm)** | **Max Torque (Nm)** |
|---|---|---|---|---|---|
| Blue Canyon Technologies | RWP015 | 0.015 | 0.130 | 42 x 42 x 19 | 0.004 |
| Blue Canyon Technologies | RWP050 | 0.050 | 0.24 | 58 x 58 x 25 | 0.007 |
| Blue Canyon Technologies | RWP100 | 0.10 | 0.33 | 70 x 70 x 25 | 0.007 |
| Blue Canyon Technologies | RWP500 | 0.50 | 0.75 | 110 x 110 x 38 | 0.025 |
| Blue Canyon Technologies | RW1 | 1.0 | 0.95 | 110 x 110 x 54 | 0.07 |
| Blue Canyon Technologies | RW4 | 4.0 | 3.2 | 170 x 170 x 70 | 0.25 |
| Blue Canyon Technologies | RW8 | 8.0 | 4.4 | 190 x 190 x 90 | 0.25 |
| Blue Canyon Technologies | CMG8 | 8 | 13 | 220x220x300 | 8 |
| Blue Canyon Technologies | CMG12 | 12 | 18 | 240x430x380 | 12 |
| Blue Canyon Technologies | DCE | N/A | 0.16 | 3.937x3.937x 0.5 (in) | N/A |
| AAC Clyde Space | iADCS400 | 0.06 | 1.15 to 1.7 | 95.4 x 95.9 x 67.3 | 2 |

Table 4-5 – Commercially available Attitude Control Systems [25].

| **Company** | **Model** | **Momentum Capacity (mNms)** | **Mass (kg)** | **Volume (mm)** |
|---|---|---|---|---|
| Blue Canyon Technologies | XACT-15 | 15 | 0.885 | 10x10x5 (0.5U) |
| Blue Canyon Technologies | XACT-50 | 50 | 1.23 | 10x10x7.54 (0.75U) |
| Blue Canyon Technologies | XACT-100 | 100 | 1.813 | 10x10x5 (0.5U) |
| Blue Canyon Technologies | FLEXCORE | 500-8000 | N/A | 12.1x11.4x4.9 |

Now, let's use a typical Falcon 9 flight to carry a payload that carries Starlink satellites that weigh approximately 800 kg, with about 25 satellites within the rocket's fairing. Now the simulation model will be. Where the rocket will have two stages, each with its own tanks,

Table 4-6 – SpaceX's Falcon 9 specs and payload capacity [18]

| **Height (with fairing) (m)** | **Diameter (m)** | **First-stage (kg)** | **Second-stage (kg)** | **25 Starlink V2 (kg)** | **Total mass (kg)** |
|---|---|---|---|---|---|
| 70 | 3.7 | 445,052 | 120322 | 18,400 | 583,774 |

Table 4-7 – SpaceX's Falcon 9 specs and payload capacity [18]

| **First-stage engines** | **First-stage propellant mass (kg)** | **Second-stage engines** | **Second-stage propellant mass (kg)** | **Engine mass flow rate (kg/s)** |
|---|---|---|---|---|
| 9 | 395,700 | 1 | 92,670 | 266.89 – 301.13 |

# 5. Modeling of an In-flight Rocket Booster

Now that the hardware selection with requirements is completed, let's start modeling the system. The first need-to-know equation should be the Tsiolkovsky rocket equation or ideal rocket equation that calculates the change in the rocket's velocity, which can be formulated from an equivalent velocity and the change in the rocket's mass as follows:

$$\Delta v = v_e \ln\left(\frac{m_e}{m_f}\right) = g_0 I_{sp} \ln\left(\frac{m_e}{m_f}\right) \quad (5.1)$$

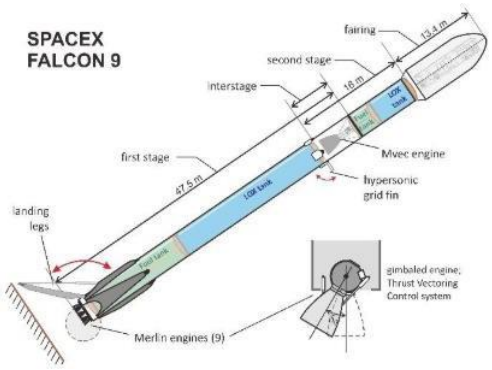


Figure 5-1 – SpaceX's Falcon 9 rocket booster and Merlin, gimbaled rocket engines [4].

Similar to Chapter 2 and Chapter 3, in order to begin modeling the rocket. Firstly, drag would be applied to the body of the rocket, in addition to gravitational force and thrust force. The effect of Coriolis force also exists and applies directly on the rocket airframe.

The goal of the simulation will be to design an attitude control system for attitude (pitch/yaw) angle $\theta = 90°$ of a multi-state Falcon-style rocket booster. Analyzing the dynamical state of the system is required by deriving the governing equations of motion for the given rocket booster. The attitude position of the rocket $\theta$ can be controlled by the thrust force $F_T$ with either a max $5°$ gimbal angle for the first-stage engines and $15°$ angle for the second-stage engine.

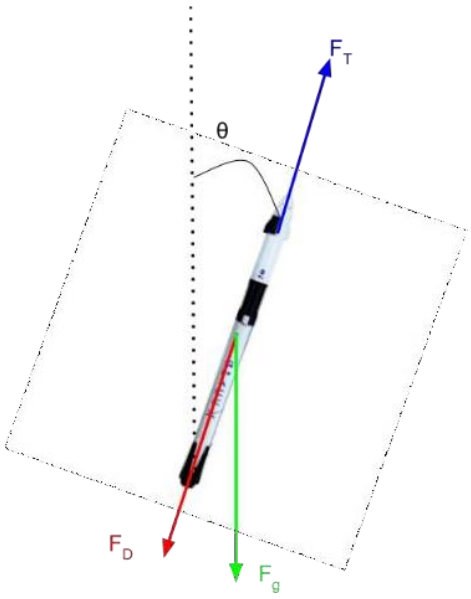


Figure 5-2 Simulation model for the rocket

Firstly, let's take a look at the de-rolled body frame of the rocket with the Newton 2nd law as follows, as up and to the right are positive axes:

$$\vec{F_T} + \vec{F_D} + \vec{F_g} = M\,a \tag{5.2}$$

Or,

$$F_T = F_D + Mgcos\theta + M\,a \tag{5.3}$$

The booster thrust can be calculated differently as an equation of pressure, velocity, and mass flow rate:

$$F_T = \dot{m}_1 v_e + (p_e - p_a)A_e \tag{5.4}$$

Where $\dot{m}_1$ is the mass flow rate of the first stage, $p_e$ is exit pressure and $p_a$ is ambient pressure of the environment, while $A_e$ is the exit area of the nozzle. Therefore, by substituting $F_T$ from *(5.3)* into *(5.4)* would result in:

$$\dot{m}_1 v_e + (p_e - p_a)A_e = F_D + Mgcos\theta + M\,a \tag{5.5}$$

Drag force applied on the rocket airframe can also be calculated as an equation of air density, drag coefficient, current velocity, and total surface area as:

$$F_D = \frac{1}{2}\rho V^2 C_D A \tag{5.6}$$

Therefore, *(5.5)* becomes:

$$\dot{m}_1 \vec{v}_e + (p_e - p_a)A_e = \frac{1}{2}\rho V^2 C_D A + Mg\cos\theta + M\,a \qquad (5.7)$$

However, it is worth noticing that mass M of the entire rocket is the sum of both stages' mass whereas before the separation of the first stage, the mass $m_1$ of the booster changes over time. Therefore, *(5.7)* can be rewritten as:

$$(m_1 + m_2)a = F_T - \frac{1}{2}\rho V^2 C_D A - (m_1 + m_2)g\cos\theta \qquad (5.8)$$

$$\frac{d((m_1(t)+m_2)v(t))}{dt} = F_T(t) - \frac{1}{2}\rho v(t)^2 C_D A - (m_1(t) + m_2)g\cos\theta \qquad (5.9)$$

$$v(t)\frac{d(m_1(t))}{dt} + (m_1(t) + m_2)\frac{d(v(t))}{dt} = F_T(t) - \frac{1}{2}\rho v(t)^2 C_D A - (m_1(t) + m_2)g\cos\theta \qquad (5.10)$$

As thrust is defined in *(5.4)*, however, with an ideal thrust equation, building a model based on the idea of flight conditions can be defined as:

$$F_T = \dot{m}_1 v_e \qquad (5.11)$$

Or can be rewritten to match with the format of *(5.8)*, *(5.9)*, and *(5.10)* a derivative of time as follows:

$$F_T = \frac{d(m_1(t))}{dt} v_e \qquad (5.12)$$

Now the ideal thrust equation, substitute the thrust force from *(5.12)* into *(5.10)* to achieve:

$$v(t)\frac{d(m_1(t))}{dt} + (m_1(t) + m_2)\frac{d(v(t))}{dt} = \frac{d(m_1(t))}{dt} v_e - \frac{1}{2}\rho v(t)^2 C_D A - (m_1(t) + m_2)g\cos\theta \qquad (5.13)$$

Notice, since this is before the separation of the first stage, the engine of the second stage is not yet burning, therefore $m_2$ is still a constant.

Simplifying *(5.13)* as follows:

$$(m_1(t) + m_2)\frac{d(v(t))}{dt} - \frac{d(m_1(t))}{dt}(v(t) - v_e) + \frac{1}{2}\rho v(t)^2 C_D A + (m_1(t) + m_2)g\cos\theta = 0 \qquad (5.14)$$

*(5.14)* results in an equation of Riccati different equation. In order to solve this, the Differential Transform Method or DTM needed to be mentioned and used.

DTM uses Taylor's series expansive, which has been utilized to solve nonlinear systems or any system that contains oscillation. The Differential Transform Method is fit for solving nonlinear ordinary equations without the need for discretizing.

Table 5-1 – Deferential Transform Method [22]

| **Original Function** | **Transformed Function** |
|---|---|
| $x(t) = \alpha f(x) \pm \beta g(t)$ | $X(k) = \alpha F(k) \pm \beta G(k)$ |
| $x(t) = \frac{d^m f(t)}{dt^m}$ | $X(k) = \frac{(k+m)!\, F(k+m)}{k!}$ |
| $x(t) = f(t)g(t)$ | $X(k) = \sum_{l=0}^{k} F(l)G(k-l)$ |
| $x(t) = t^m$ | $X(k) = \delta(k-m) = \begin{cases} 1, if\ k = m \\ 0\ if\ k \neq m \end{cases}$ |
| $x(t) = e(t)$ | $X(k) = \frac{1}{k!}$ |
| $x(t) = \sin(\omega t + \alpha)$ | $X(k) = \frac{\omega^k}{k!} \sin(\frac{k\pi}{2} + \alpha)$ |
| $x(t) = \sin(\omega t + \alpha)$ | $X(k) = \frac{\omega^k}{k!} \cos(\frac{k\pi}{2} + \alpha)$ |

Applying the Differential Transform Method into *(5.14)* with the initial conditional of at t = 0, the rocket booster would then have close to zero velocity and $m_1$ would be dry mass of the booster combined with the propellant's mass of the first stage for:

$$(m_1(t) + m_2)V(k) - M(k)(-v_e) + (m_1(t) + m_2)gcos\theta = 0 \qquad (5.15)$$

$$(m_1(t) + m_2)(k+1)V(k+1) - (k+1)M(k+1)(-v_e) + (m_1(t) + m_2)gcos\theta = 0 \qquad (5.16)$$

Next, analyzing the dynamic state of the system is required by deriving the governing equations of motion for the given inverted pendulum system. The attitude position of the pendulum $\theta$ is controlled by providing an applied force F [N] onto the cart on the horizontal plan x [m] while under the influence of gravity with gravitational acceleration g [m/s$^2$].

Beginning with the cart, analyzing the free-body diagram of the cart for the combination of forces, the equation of motion is as follows:

$$\vec{F}_D + \vec{F}_T + F_g = M\,a \tag{5.17}$$

Where $\vec{F}_R$ is the reaction force from the pendulum onto the cart, $\vec{F}_A$ is the applied force onto the booster to assist attitude control for the pendulum, $\vec{F}_N$ is the normal force of the ground onto the booster and $\vec{F}_A$ is the gravitational force applied to the booster while $\ddot{x}$ is the acceleration of the booster. However, only forces in the x-direction would have a meaningful impact on the booster's acceleration. In addition, to make it easier moving forward, the reaction $\vec{F}_R$ will be written as $F^C_x$ and $F^C_y$ when broken down into components for the x-axis and the y-axis, hence, *(3.1)* is rewritten to isolate the forces in the x-plane of the system as follows:

$$\vec{F}^C_A + \vec{F}^C_R = M\,a \tag{5.18}$$

Or as,

$$F^C_A + F^C_x = M\ddot{x} \tag{5.19}$$

Where $\ddot{x}$ represents the acceleration the booster would experience under the combined forces in the x-direction. Next, the second element of the system, summing up the net forces applying to the inverted pendulum as follows:

$$\vec{F}^P_R + \vec{F}^P_g = m\vec{\ddot{a}}_P \tag{5.20}$$

Noticing in *(3.2)* and *(3.4)*, the booster and the pendulum would be experiencing different accelerations, $a$ and $\vec{\ddot{a}}_P$. Now in a similar fashion, isolating the y-direction and x-direction forces as follows:

$$F^P_y - F^P_g = m\ddot{y_P} \tag{5.21}$$

And,

$$F^P_x = m\ddot{x_P} \tag{5.22}$$

Where $\vec{F}^{P}_{R}$ is the reaction force of the booster onto the pendulum. Similar to $\vec{F}^{C}_{R}$, $\vec{F}^{C}_{R}$ will also be broken down into $F^{P}_{x}$ while referring to the x component of the reaction force from the booster onto the pendulum $F^{P}_{y}$ while referencing the y component of the reaction force. Now to unify *(3.5)* and *(3.6)*, the acceleration the pendulum would experience can be addressed in an equation of the booster's acceleration as follows:

$$x_p = x + Lsin\theta \tag{5.23}$$

Taking the derivative of *(3.7)* with respect to time:

$$\dot{x_P} = \dot{x} + L\dot{\theta}cos\theta \tag{5.24}$$

To achieve the pendulum's acceleration, take the derivative of *(3.8)* with respect to time as follows:

$$\ddot{x_P} = \ddot{x} + L\ddot{\theta}cos\theta - L\dot{\theta}^2 sin\theta \tag{5.25}$$

In a similar fashion, $y_p$ can be derived as:

$$y_p = Lcos\theta \tag{5.26}$$

Taking the derivative of *(3.10)* with respect to time:

$$\dot{y_P} = -L\dot{\theta}sin\theta \tag{5.27}$$

To achieve the pendulum's acceleration, take the derivative of *(3.8)* with respect to time as follows:

$$\ddot{y_P} = -L\ddot{\theta}sin\theta + L\dot{\theta}^2 cos\theta \tag{5.28}$$

Now substitute *(3.9)* and into *(3.6)* for:

$$F^{P}_{x} = m\ddot{x} + mL\ddot{\theta}cos\theta - mL\dot{\theta}^2 sin\theta \tag{5.29}$$

According to Newton's third law of motion, when two objects interact, they apply forces of equal magnitude and opposite directions to each other. Hence, the reaction forces of the booster and the pendulum onto each other are equal:

$$F^{P}_{x} = -F^{C}_{x} \tag{5.30}$$

Combining *(3.11)* and *(3.3)* results in the first equation of motion for the overall system of an inverted pendulum on a booster as follows:

$$F^{C}_{A} - m\ddot{x} - mL\ddot{\theta}cos\theta + mL\dot{\theta}^2 sin\theta = M\ddot{x}$$

$$F^{C}_{A} = M\ddot{x} + m\ddot{x} + mL\ddot{\theta}cos\theta - mL\dot{\theta}^2 sin\theta$$

$$F^{C}_{A} = (M + m)\ddot{x} + mL(\ddot{\theta}cos\theta - \dot{\theta^2}\ sin\theta) \quad (5.31)$$

Due to this being non-linearized, the dynamical system can be linearized with small angle approximation in *(2.15)* with the assumption that controlled angle $\theta$ would only stay in a small neighborhood of around $0^o$ as that is the goal of the system, is to keep the pendulum vertically upright at an angle of $90^o$.

$$cosx \approx 1 \quad (5.32)$$

And,

$$\dot{\theta^2} \approx 0 \quad (5.33)$$

Hence if assign $F^{C}_{A}$ to u as the control input vector, and the first 3 stages of the state vector is $\begin{bmatrix} \theta \\ \dot{\theta} \\ \ddot{x} \end{bmatrix}$. Thus, the nonlinear pendulum dynamical system linearized with small angle approximation as:

$$(M + m)\ddot{x} + mL\ddot{\theta} = u \quad (5.34)$$

Let's take a look at the forces applied on the pendulum in the y-direction from *(3.5)* as the pendulum is under the influence of the reaction force from the booster and the gravitational force and substitute the y-direction acceleration acquired from *(3.12)* as follows:

$$F^{P}_{y} - F^{P}_{g} = m(-L\ddot{\theta}sin\theta + L\dot{\theta^2}\ cos\theta)$$

$$F^{P}_{y} - mg = m(-L\ddot{\theta}sin\theta + L\dot{\theta^2}\ cos\theta) \quad (5.35)$$

As specified before, $F^{P}_{x}$ and $F^{P}_{y}$ are the horizontal and vertical components of the reaction applied on the pendulum from the rolling booster. Therefore, they can be derived as the function of the reaction force as follows:

$$F^{P}_{x}\hat{\imath} = \vec{F^{P}}_{R}sin\theta \quad (5.36)$$

With the magnitude of:

$$F^{P}_{x} = |\vec{F^{P}}_{R}|sin\theta \quad (5.37)$$

And,

$$F^{P}_{y}\hat{\jmath} = \vec{F^{P}}_{R}cos\theta \quad (5.38)$$

Magnitude of:

$$F^P{}_y = |\overrightarrow{\overrightarrow{F^P}}_R| cos\theta \quad (5.39)$$

Now, substitute $F^P{}_x$ acquired from *(3.21)* into *(3.11)*, and $F^P{}_y$ acquired from *(3.23)* into *(3.13)* to get:

$$|\overrightarrow{\overrightarrow{F^P}}_R| sin\theta = m\ddot{x} + mL\ddot{\theta} cos\theta - mL\dot{\theta^2}\ sin\theta \quad (5.40)$$

And,

$$|\overrightarrow{\overrightarrow{F^P}}_R|\ cos\theta - mg = m(-L\ddot{\theta} sin\theta - L\dot{\theta^2}\ cos\theta) \quad (5.41)$$

Now, multiply $cos\theta$ to *(3.22)* and $sin\theta$ to *(3.23)* for the next step:

$$|\overrightarrow{\overrightarrow{F^P}}_R| sin\theta cos\theta = m\ddot{x} cos\theta + mL\ddot{\theta}(cos\theta)^2 - mL\dot{\theta^2}\ sin\theta cos\theta \quad (5.42)$$

And,

$$|\overrightarrow{\overrightarrow{F^P}}_R|\ cos\theta sin\theta - mgsin\theta = -mL\dot{\theta^2}\ cos\theta sin\theta - mL\ddot{\theta}(sin\theta)^2 \quad (5.43)$$

Subtract *(3.25)* from *(3.24)* for the left-hand side:

$$|\overrightarrow{\overrightarrow{F^P}}_R|\ sin\theta cos\theta - |\overrightarrow{\overrightarrow{F^P}}_R\ |\ cos\theta sin\theta + mgsin\theta$$

$$mgsin\theta \quad (5.44)$$

The right-hand side of the equation is:

$$m\ddot{x} cos\theta + mL\ddot{\theta}(cos\theta)^2 - mL\dot{\theta^2}\ sin\theta cos\theta + mL\dot{\theta^2}\ cos\theta sin\theta + mL\ddot{\theta}(sin\theta)^2$$

$$m\ddot{x} cos\theta + mL\ddot{\theta} \quad (5.45)$$

Therefore, as the result of combining the left-hand side and the right-hand side of the equation as follows:

$$mgsin\theta = m\ddot{x} cos\theta + mL\ddot{\theta} \quad (5.46)$$

Similarly, linearized *(3.28)* in the same process with *(2.13)*, *(3.16)*, and *(3.17)* as in *(3.18)* to result:

$$mg\theta = m\ddot{x} + mL\ddot{\theta} \quad (5.47)$$

Or,

$$g\theta = \ddot{x} + L\ddot{\theta} \quad (5.48)$$

Now, with *(3.30)*, the second governing equation of motion for the system is introduced. However, it must be pointed out that, *(3.30)* is only qualified as the second governing equation for the system due to the fact that this simulation model uses a uniform point mass sphere placed on top of a massless inverted pendulum. Hence all the mass is not uniformly distributed but is concentrated in the top end of the pendulum. Therefore, it is possible to ignore the moment of inertia that then would possibly exist on a uniformly distributed pendulum rod rotating about it fixed point at the lower end of the rod. A scenario where the pendulum is a uniformly distributed rod would also be derived below to show the comparison between two different condition setups for the differences.

Now the overall system can be represented as:

$$\begin{cases} (M+m)\ddot{x} + mL\ddot{\theta} = u \\ g\theta = \ddot{x} + L\ddot{\theta} \end{cases} \tag{5.49}$$

However, *(3.31)* contains two equations that are coupled together. Therefore, it would be necessary to further decouple them, and now return to (*3.29)*, before simplifying mass m [kg] out of the equation to achieve *(3.30)*, by isolating $mL\ddot{\theta}$ in (*3.18)* and *(3.29)* for:

$$\begin{cases} mL\ddot{\theta} = u - (M+m)\ddot{x} \\ mL\ddot{\theta} = m\ddot{x} - mg\theta \end{cases} \tag{5.50}$$

Therefore, *(3.32)* would result in the first decoupled governing equation of motion for the system as:

$$u - (M+m)\ddot{x} = m\ddot{x} - mg\theta$$

$$M\ddot{x} = u - mg\theta \tag{5.51}$$

In a similar fashion to *(3.33)*, to decouple *(3.18)*, isolating the term $\ddot{x}$ in (*3.30)* to create a similar equation as:

$$\ddot{x} = L\ddot{\theta} - g\theta \tag{5.52}$$

Now substituting *(3.34)* into *(3.18)* to acquire the other decoupled governing equation of motion of the system as follows:

$$(M+m)(L\ddot{\theta} - g\theta) + mL\ddot{\theta} = u$$

$$mL\ddot{\theta} = (M+m)g\theta - u \tag{5.53}$$

Hence, the simulation model of the system with the second order, linearized and decoupled is as follows:

$$\begin{cases} M\ddot{x} = -mg\theta + u \\ mL\theta = (M+m)g\theta - u \end{cases} \quad (5.54)$$

Isolating $\ddot{x}$ and $\theta$ for:

$$\begin{cases} \ddot{x} = \frac{-mg}{M}\theta + \frac{1}{M}u \\ \theta = \frac{(M+m)g}{mL}\theta - \frac{1}{mL}u \end{cases} \quad (5.55)$$

Let $x$ be $x_1$, $\dot{x}$ be $x_2$ or $\dot{x}_1$, then $\ddot{x}$ would be $\dot{x}_2$, and $\theta$ be $x_3$, $\theta$ be $x_4$ or $\dot{x}_3$, then $\theta$ would be $\dot{x}_4$, where $\begin{bmatrix} x_1 \\ x_2 \\ x_3 \\ x_4 \end{bmatrix} = \begin{bmatrix} x \\ \dot{x} \\ \theta \\ \theta \end{bmatrix}$ is the state vector, and vector u is the control input vector.

Therefore, the open-loop linearized state-space system of the inverted pendulum about its unstable equilibrium point is:

$$\begin{bmatrix} \dot{x}_1 \\ \dot{x}_2 \\ \dot{x}_3 \\ \dot{x}_4 \end{bmatrix} = \begin{bmatrix} 0 & 1 & 0 & 0 \\ 0 & 0 & \frac{-mg}{M} & 0 \\ 0 & 0 & 0 & 1 \\ 0 & 0 & \frac{(m+M)g}{mL} & 0 \end{bmatrix} \begin{bmatrix} x_1 \\ x_2 \\ x_3 \\ x_4 \end{bmatrix} + \begin{bmatrix} 0 \\ \frac{1}{M} \\ 0 \\ -\frac{1}{mL} \end{bmatrix} u \quad (5.56)$$

Meanwhile, state and output equations can be expressed as:

$$\begin{cases} \dot{x} = Ax + B\vec{u} \\ y = C\,x + D\vec{u} \end{cases} \quad (5.57)$$

Where A is the state matrix, B is the input matrix, C is the output matrix and D is the feedforward matrix. Therefore, A = $\begin{bmatrix} 0 & 1 & 0 & 0 \\ 0 & 0 & \frac{-mg}{M} & 0 \\ 0 & 0 & 0 & 1 \\ 0 & 0 & \frac{(m+M)g}{mL} & 0 \end{bmatrix}$, B = $\begin{bmatrix} 0 \\ \frac{1}{M} \\ 0 \\ -\frac{1}{mL} \end{bmatrix}$, C = [0 0 1 0], since the only interested output is the attitude angle y = $\theta$, and no feedforward matrix. From *(5.55)*, the transfer function of the open-loop system can be done via the Lagrange transform on both sides of the equal sign as:

$$\mathcal{L}(\theta) = \mathcal{L}\left[\frac{(M+m)g}{mL}\theta - \frac{1}{mL}u(s)\right]$$

$$s^2\theta(s) = \frac{(M+m)g}{mL}\theta(s) - \frac{1}{mL}u(s)$$

$$\frac{\theta(s)}{u(s)} = \frac{-\frac{1}{mL}}{s^2 - \frac{(M+m)g}{mL}} \qquad (5.58)$$

Checking the controllability of the system with the controllability matrix Co can be defined as:

$$Co = [B \quad AB \quad A^2B \quad \cdots \quad A^{(n-1)}B] \qquad (5.59)$$

Where A is still the state matrix while B is still the input matrix, and "n" is the number of states, in this particular system, n is 4. Therefore, the controllability matrix can be achieved from *(3.41)* as follows:

$$Co = [B \quad AB \quad A^2B \quad A^3B] \qquad (5.60)$$

Calculating the components of the controllability matrix, $AB$:

$$AB = \begin{bmatrix} 0 & 1 & 0 & 0 \\ 0 & 0 & \frac{-mg}{M} & 0 \\ 0 & 0 & 0 & 1 \\ 0 & 0 & \frac{(m+M)g}{mL} & 0 \end{bmatrix} \begin{bmatrix} 0 \\ \frac{1}{M} \\ 0 \\ -\frac{1}{mL} \end{bmatrix} = \begin{bmatrix} \frac{-mg}{M} \\ 0 \\ 0 \\ 0 \end{bmatrix} \qquad (5.61)$$

Calculating $A^2B$:

$$A^2B = \begin{bmatrix} 0 & 1 & 0 & 0 \\ 0 & 0 & \frac{-mg}{M} & 0 \\ 0 & 0 & 0 & 1 \\ 0 & 0 & \frac{(m+M)g}{mL} & 0 \end{bmatrix}^2 \begin{bmatrix} 0 \\ \frac{1}{M} \\ 0 \\ -\frac{1}{mL} \end{bmatrix} = \begin{bmatrix} 0 \\ \frac{g}{ML} \\ 0 \\ \frac{-(m+M)g}{(mL)^2} \end{bmatrix} \qquad (5.62)$$

Calculating $A^3B$:

$$A^3B = \begin{bmatrix} 0 & 1 & 0 & 0 \\ 0 & 0 & \frac{-mg}{M} & 0 \\ 0 & 0 & 0 & 1 \\ 0 & 0 & \frac{(m+M)g}{mL} & 0 \end{bmatrix}^3 \begin{bmatrix} 0 \\ \frac{1}{M} \\ 0 \\ -\frac{1}{mL} \end{bmatrix} = \begin{bmatrix} \frac{g}{ML} \\ 0 \\ \frac{-(m+M)g}{(mL)^2} \\ 0 \end{bmatrix} \qquad (5.63)$$

$$Co = \begin{bmatrix} 0 & \frac{-mg}{M} & 0 & \frac{g}{ML} \\ \frac{1}{M} & 0 & \frac{g}{ML} & 0 \\ 0 & 0 & 0 & \frac{-(m+M)g}{(mL)^2} \\ -\frac{1}{mL} & 0 & \frac{-(m+M)g}{(mL)^2} & 0 \end{bmatrix} \quad (5.64)$$

Now, to determine whether the system is fully controllable or not via taking the Rank of the controllability matrix, resulting in:

$$Rank(Co) = 4 \quad (5.65)$$

The system is fully controllable as it is full rank. In addition, this can also be determined by observing the presence of input control vector u in both governing equations of motion of the system.

To simulate the model, parameters need to be assigned for the booster's mass. M = 3 [kg], the mass of the sphere located on top of the inverted pendulum, m = 1 [kg], the length of the massless inverted pendulum, L = 1 [m], while gravitational acceleration is g = 9.81 [kg/s$^2$]. For initializing the system with the initial conditions of $x_i = \begin{bmatrix} x_1 \\ x_2 \\ x_3 \\ x_4 \end{bmatrix} = \begin{bmatrix} x \\ \dot{x} \\ \theta \\ \dot{\theta} \end{bmatrix} = \begin{bmatrix} 0 \\ 0 \\ 0.01 \\ 0 \end{bmatrix}$, where the booster would start at the origin, with no velocity, while the pendulum is set to be slightly off-set to the equilibrium of 0-degree angle and has no angular velocity.

Now, with the initial position given as the starting state of the system, the desired state of the system can be $x_f = \begin{bmatrix} x_1 \\ x_2 \\ x_3 \\ x_4 \end{bmatrix} = \begin{bmatrix} x \\ \dot{x} \\ \theta \\ \dot{\theta} \end{bmatrix} = \begin{bmatrix} 1 \\ 0 \\ 0 \\ 0 \end{bmatrix}$, where the final position is an arbitrary location away from the origin, in this case, is 1, while not translational and angular velocity residue is wanted and the inverted pendulum to stay fully upward at an angle $\theta = 0$.

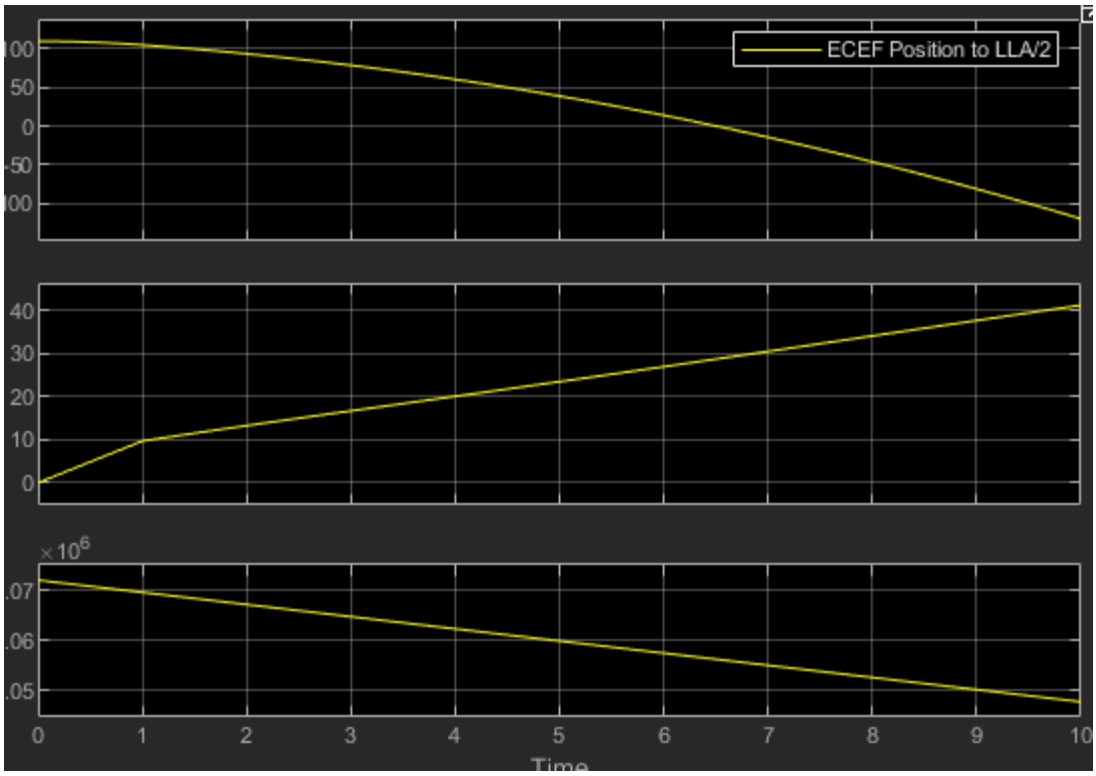


Figure 5-3 Altitude, Velocity, and Mass of the booster

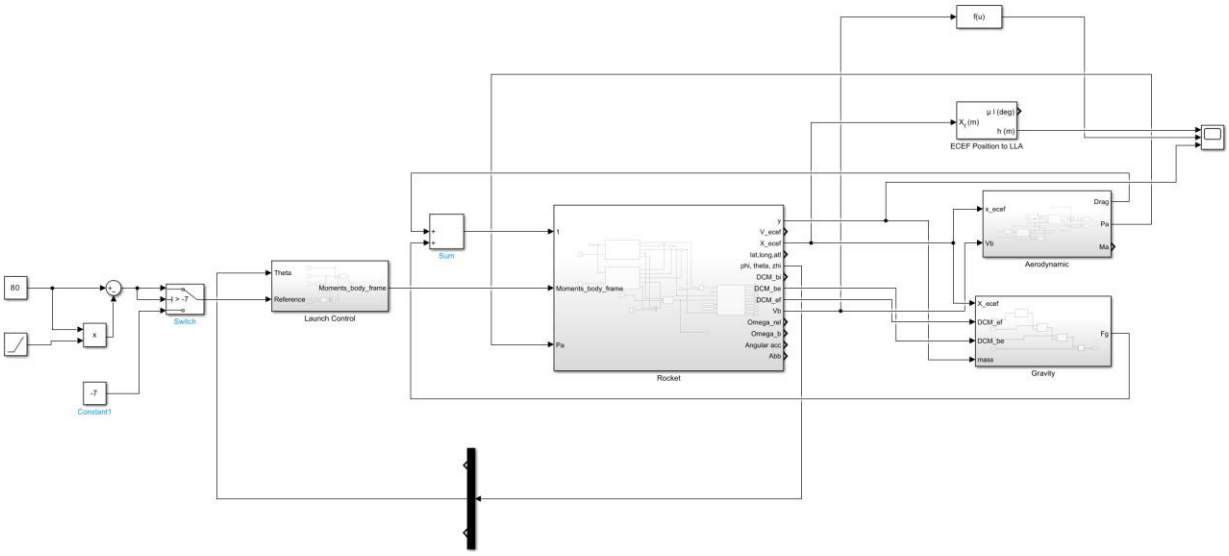


Figure 5-4 Simulation model of the booster

# 6. Conclusion and Path Forward

This project provided great experience with the successful implementation designing of attitude control along with the creation of a mathematical model for various dynamic systems. The project has demonstrated the effectiveness of the designed system in meeting the project's objectives. Through meticulous planning, rigorous testing, and iterative refinements, we achieved reliable performance, operational efficiency, and compliance with the specified requirements. The system has been validated to function consistently under expected operating conditions, ensuring enhanced reliability and control. However, throughout the project, various assumptions had to be made, which is a good engineering tool, but assumptions also significantly remove the complexity of the problems.

The path forward from here is to design a better control system for the rocket booster with higher fidelity and fewer assumptions. Implementing better tools of control like the Kalman filter is a great way to improve the knowledge in the subject. For a better simulation model, it can be good to look into better and more dynamic environment block, gain scheduling with table look-up for different flight conditions.

# References


[1] Jenie, Y. I., Suarjaya, W. W. H., and Poetro, R. E., "Falcon 9 Rocket Launch Modeling and Simulation with Thrust Vectoring Control and Scheduling," *2019 IEEE 6th Asian Conference on Defence Technology (ACDT)*, pp. 25-31, 2019.

[2] Sallam, A. M. F., Makled, A. E. S, "Two-Stage Launch Vehicle Trajectory Modeling for Low Earth Orbit Applications," *World Academy of Science, Engineering and Technology International Journal of Aerospace and Mechanical Engineering*, vol. 11, no. 1, pp. 86-93, 2017

[3] Fu, B., Xu, J., and Zhang, D., "Modeling and Analysis of Long Booster Clustered Launch-Vehicle," *Scientific Reports*, vol. 10, no. 1611, 2020. Retrieved 3 May 2024 from https://doi.org/10.1038/s41598-020-58173-6

[4] Kana, D. D., Ko, W. L., Francis, P. H. and Nagy, A., "Coupling between Structure and Liquid Propellants in a Parallel-Stage Space Shuttle Design," *Journal of Spacecraft and Rockets*, vol. 9, no. 11, 1972.

[5] Sayar, B. A. and Baumgarten, J. R., "Linear and Nonlinear Analysis of Fluid Slosh Dampers" *AIAA Journal*, vol. 20, no. 11, pp. 1534-1538, 1982.

[6] Du, W., Wie, B. and Whorton M., "Dynamic Modeling and Control Simulation of Large Flexible Launch Vehicles," *AIAA Guidance, Navigation, and Control Conference*, Honolulu, Hawaii, 2008. Retrieved 3 May 2024 from https://arc.aiaa.org/doi/abs/10.2514/6.2008-6620

[7] Tewari, A., "Atmospheric and Space Flight Dynamics-Modeling and Simulation with MATLAB and SIMULINK," Birkhauser, Boston, 2006, Chaps 4-7.

[8] dos Santos, P. and Oliveira, P., "Thrust vector control and state estimation architecture for low-cost small-scale launchers," *Universidade de Lisboa, Av. Rovisco Pais 1, 1049-001*, Lisbon, Portugal, 2023

[9] Jang, J. W., Alaniz, A., Hall, R., Bedrossian, N., Hall, C. and Jackson, M., "Design of launch vehicle flight control systems using ascent vehicle stability analysis tool," *AIAA Guidance, Navigation, and Control Conference*, Portland, Oregon, 2019.

[10] Lu, B., Falde, D., Iriarte, E. and Besnard, E., "Switching robust control for a nanosatellite launch vehicle," *Aerospace Science and Technology*, vol. 42, pp. 259-266, 2015.

[11] Wie, B., Du, W., and Whorton M., "Analysis and Design of Launch Vehicle Flight Control System," *AIAA Guidance, Navigation, and Control Conference*, Honolulu, Hawaii, 2008.

[12] Sopegno, L., Liverri, P., Stefanovic, M. and Valavanis, P., "Linear Quadratic Regulator: A Simple Thrust Vector Control System For Rocket," *30th Mediterranean Conference on Control and Automation (MED)*, Vouliagmeni, Greece, 2022.

[13] Kisabo, A., Adebimpe, A. and Samuel, S., "Pitch Control of a Rocket with a Novel LQR/LTR Control Algorithm," *Journal of Aircraft and Spacecraft Technology*, vol. 3, no. 1, pp. 24-37, 2019.

[14] D'Amico, S., Gagg Filho, F., and Parisi, L., "Enhanced Attitude Determination Using Integrated Star Trackers and Extended Kalman Filtering." *Spacecraft Systems Engineering*, vol 45, pp. 78-92, 2022.

[15] Hassan, I. H. A., "Application to differential transformation method for solving systems of differential equations," Applied Mathematical Modeling, Vol. 32, No. 12, 2008, pp. 2552-2559. doi: 10.1016/j.apm.2007.09.025

[16] Roberts B., Sam A., Brand J., and Elliott T., "Comparative Analysis and Justification of Optimal Rocket Motor Selection in NASA USLI by Applying Newton's Second Law to a Variable Mass Body", AIAA P&E 2019. https://doi.org/10.2514/6.2019-4138

# Appendix A

# MATLAB Code

```
clear all
close all
clc

% Parameters
m = 1;
L = 1;
g = 9.81;

A = [ 0    1;
      g/L  0];

B = [0;
     1/(m*L^2)];

C = [1 0];

D = 0;

Q = diag([2000 22]);
R = 0.22;

K = lqr(A,B,Q,R);

open_system('lqrmodel');
sim('lqrmodel.slx');
```

```
m = 1;
M = 3;
L = 1;
g = 9.81;
d = 0;

A = [0 1 0 0;
     0 0 (-(m*g)/M) 0;
     0 0 0 1;
     0 0 ((m+M)*g)/(m*L) 0];

B = [0; (1/M); 0; (-1/(m*L))];

lambda = eig(A)
rank(ctrb(A,B))
```

```
lambda =

         0
         0
    6.2642
   -6.2642


ans =

     4
```

```
clear all, close all, clc
m = 2;
M = 5;
L = 3;
g = 9.81;
d = 0; % No drags

A = [0 1 0 0;
     0 0 (-(m*g)/M) 0;
     0 0 0 1;
     0 0 ((m+M)*g)/(m*L) 0];

B = [0; (1/M); 0; (-1/(m*L))];
```

```
Q = [1 0 0 0;
     0 1 0 0;
     0 0 10 0;
     0 0 0 1000];
R = .005;
K = lqr(A,B,Q,R);
```

```
ts = 0:.01:30;
xi = [0; 0; 0.1; 0];
xf = [1; 0; 0; 0];
u=@(x)-K*(x - xf);
[t,x] = ode45(@(t,x) pendoncart(x,m,M,L,g,d,u(x)),ts,x0);
```

```
function dx = pendoncart(x,m,M,L,g,d,u)
Sx = sin(x(3));
Cx = cos(x(3));
```

```
D = m*(L^2)*(M+m*(1-Cx^2));

dx(1,1) = x(2);
dx(2,1) = (1/D)*(-m^2*L^2*g*Cx*Sx + m*L^2*(m*L*x(4)^2*Sx - d*x(2))) + m*L*L*(1/D)*u;
dx(3,1) = x(4);
dx(4,1) = (1/D)*((m+M)*m*g*L*Sx - m*L*Cx*(m*L*x(4)^2*Sx - d*x(2))) - m*L*Cx*(1/D)*u;
```

```
function m = fcn(m1,m2,m3,selector)
m = 0;
if selector(1) == 1
    m = m + m1;
end
if selector(2) == 1
    m = m + m2;
end
if selector(3) == 1
    m = m + m3;
end
```

```
function out = fcn(flag, emptytank,a,b)
if flag >= 1 && emptytank == 1
        out = a;
else
        out = b;
end
```

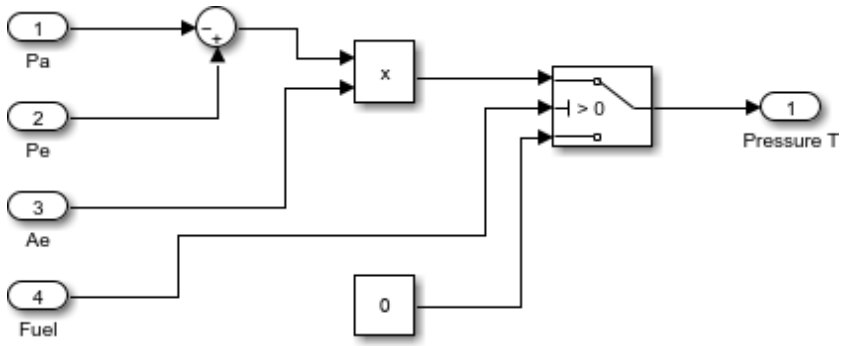

```
function g = fcn(r)
nu = 3.956004415e14;
g = -(nu/norm(r)^3).*(r);


```

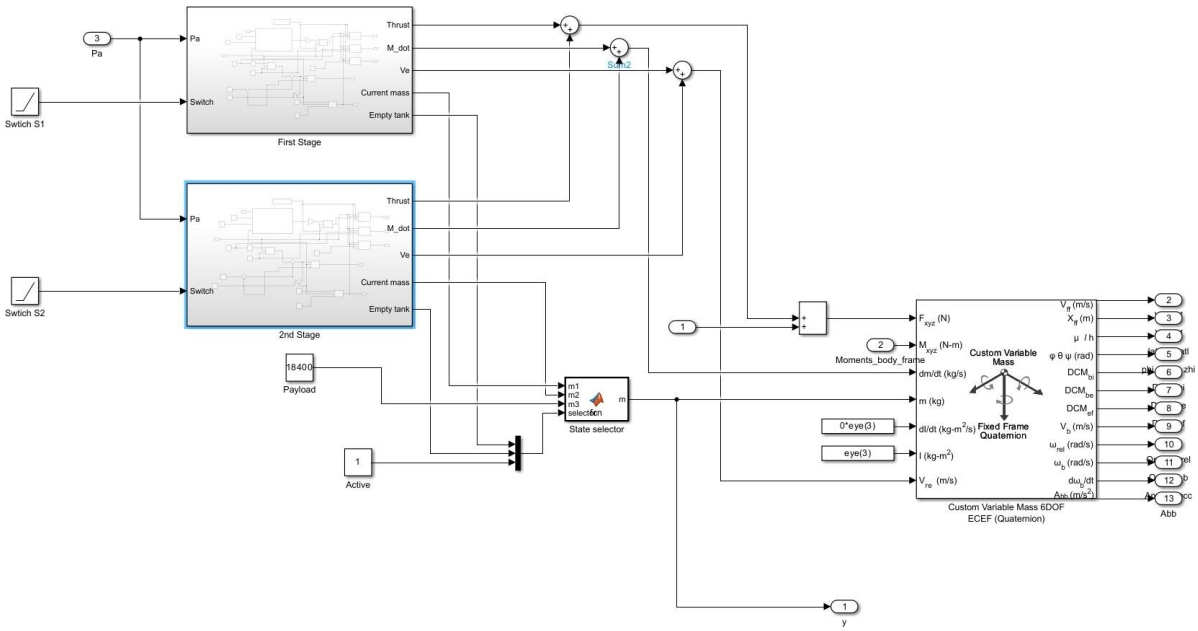


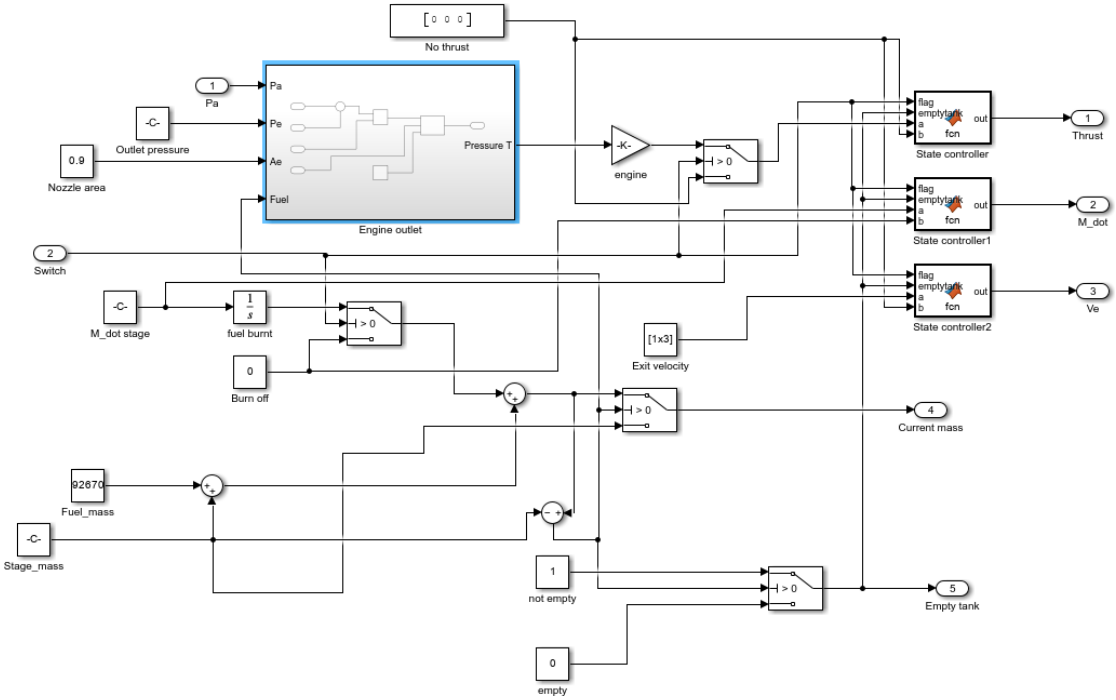

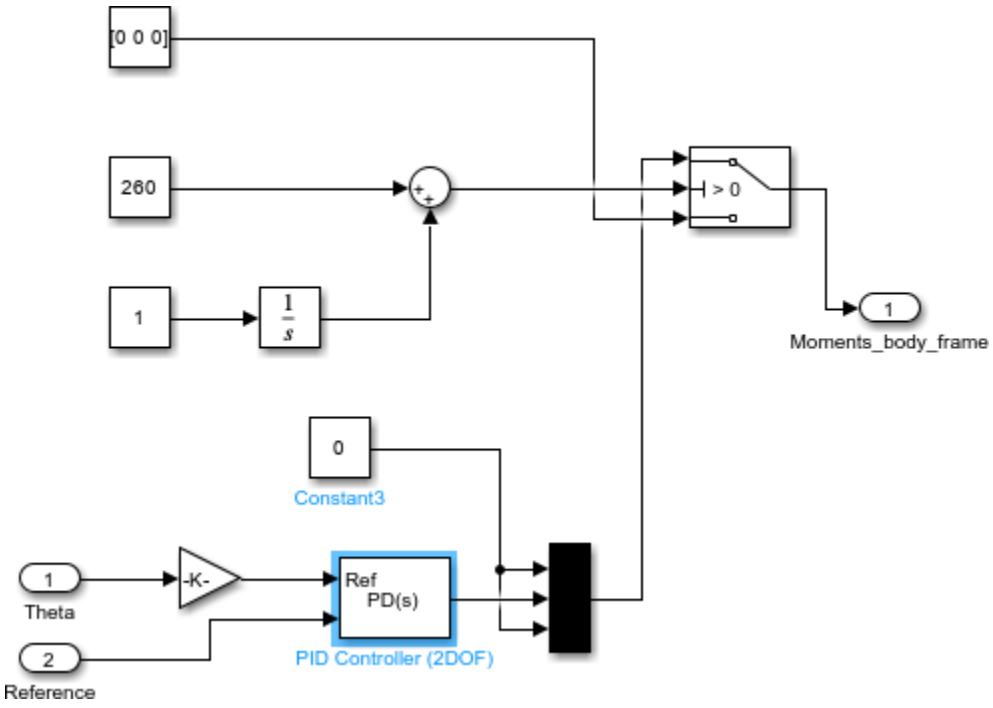


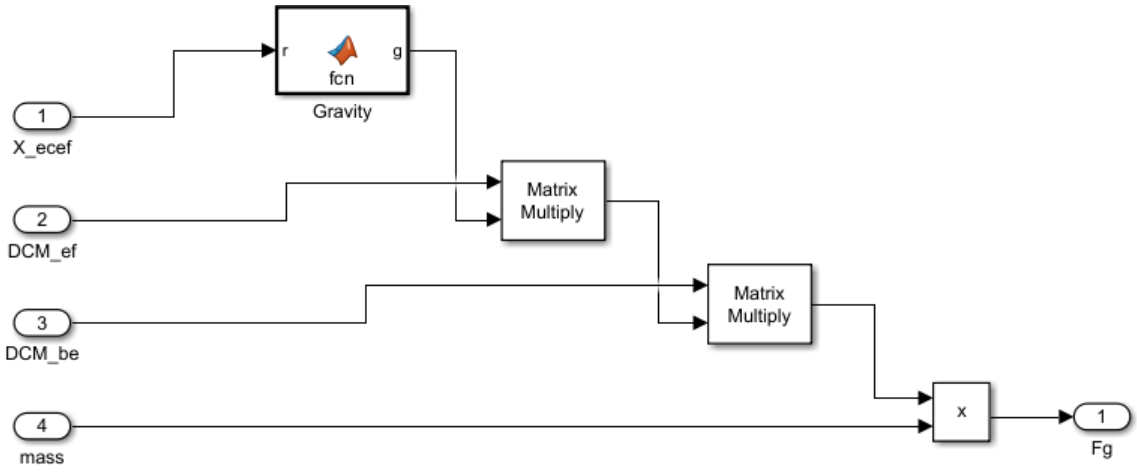


```
function g = fcn(rho,v)
g = (1/2)*rho*dot(v,v);


```

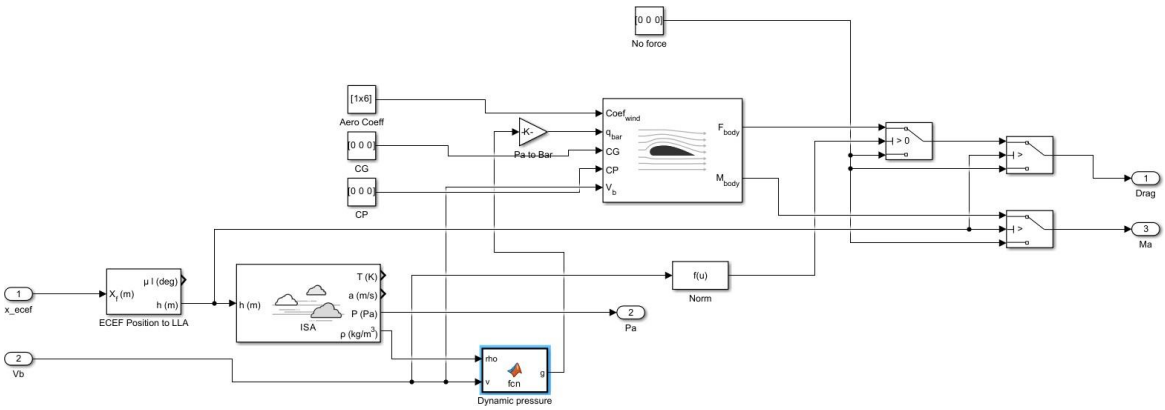
[0 0 0]
No force
[1x6]
Aero Coeff
[0 0 0]
CG
[0 0 0]
CP
-K-
Pa to Bar
Coef wind
q bar
CG
CP
V b
F body
M body
I > 0
I >
I >
1
Drag
3
Ma
1
x_ecef
μ l (deg)
X_l (m)
h (m)
ECEF Position to LLA
h (m)
ISA
T (K)
a (m/s)
P (Pa)
ρ (kg/m^3)
2
Pa
f(u)
Norm
2
Vb
rho
v
fcn
g
Dynamic pressure